5-2020

Cloning, Expression, Purification and Characterization of Heparin-binding Pocket of Recombinant FGF1

Quratulayn Ashraf
University of Arkansas, Fayetteville

Cloning, Expression, Purification and Characterization
of Heparin-binding Pocket of Recombinant FGF1

A thesis submitted in partial fulfillment
of the requirements for the degree of
Master of Science in Cell and Molecular Biology

by

Quratulayn Ashraf
Lahore University of Management Sciences
Bachelor of Science in Biology, 2012

May 2020
University of Arkansas

This thesis is approved for recommendation to the Graduate Council.

_____
Suresh Kumar Thallapuranam, Ph.D.
Thesis Chair

_____
Suresh Kumar Thallapuranam, Ph.D.
Committee Member

_____
Ravi Damodar Barabote, Ph.D.
Committee Member

_____
Paul Adams, Ph.D.
Committee Member

ABSTRACT

Fibroblast growth factors are polypeptide members of the FGF family, which to date comprises of at least 22 members. They belong to a group of growth factors and are involved in a variety of cellular processes including wound healing, angiogenesis, differentiation and development (organogenesis). Amongst FGF members, human acidic FGF-1 and basic FGF-2 are the most characterized. FGF-1 and FGF-2 are known to share more than 80% sequence similarity and have an identical structural fold. However, their biological roles are quite different. FGFs bind to heparin and heparan sulfate ligands through their heparin-binding pockets. The interactions are primarily electrostatic in nature. The heparin-binding pocket of the protein is significant in the interaction of protein with heparin. Therefore, it is important to characterize the heparin-binding pocket. This research project focuses on the characterization of heparin-binding pocket peptide of FGF1, located at the C-terminal of FGF1 (25 amino acids). To achieve this objective a fusion protein was initially created with the FGF1 C-terminal peptide fused to Rubredoxin (Rub) protein. The fused protein was expressed in BL21 (DE3) cells and purified using affinity chromatography. The FGF1 C-terminal heparin binding peptide (FGF1) was then generated by thrombin cleavage of the fused peptide and characterized by Circular Dichroism (CD), Fluorescence and Mass Spectroscopy. Characterizing the C-terminal heparin-binding region of FGF1 will aid in the understanding of the interactions involved between FGF1 and Fibroblast Growth Factor Receptors and subsequent signal transduction cascades. It will also assist in the development of agonists and antagonists of FGF1 that could potentially be used to regulate various cellular processes, both physiological and pathological. In addition, it could help in understanding the interaction of heparin with other proteins that contain the heparin-binding pocket.

ACKNOWLEDGEMENTS

I would like to thank Dr. T.K.S. Kumar, Dr. Srinivas Jayanthi, Dr. Ravi Kumar Gundampati and Musaab Al-Ameer for being excellent mentors during my time in the Kumar Lab. I would also like to extend my thanks to the rest of the members of Kumar's group for their support and encouragement.

TABLE OF CONTENTS

A. INTRODUCTION

Fibroblast growth factors (FGFs) are multifunctional polypeptide effectors, which interact with transmembrane tyrosine kinase receptors referred to as Fibroblast growth factor receptors (FGFRs) (Mohammadi, Olsen, & Ibrahimi, 2005). This interaction is mediated by heparin or heparin sulfate (HS). FGF-FGFR interaction and subsequent signal transduction result in the regulation of various cellular responses including embryonic development, adult tissue homeostasis, regenerative processes and associated tissue-specific pathologies (Kan, Wang, To, Gabriel, & McKeehan, 1996; Mohammadi et al., 2005).

More than 200 human heparin-interacting proteins have been identified to date (Ori, Free, Courty, Wilkinson, & Fernig, 2009). FGF is one of them. The structural features mediating the interactions of heparin with various proteins is an area of active research. In general, all 23 FGFs consist of 150-300 amino acids and their molecular weight is in the range 16-34-kDa (Belov & Mohammadi, 2013; Pellegrini et al., 2000). Members of the fibroblast growth factor (FGF) family of polypeptides are ubiquitous bioregulators within tissues (Kan et al., 1996). Their activity is regulated by heparan sulfates in the pericellular matrix (Kan et al., 1996).

Fibroblast growth factors (FGF) are secreted signaling proteins with diverse biological activities including embryonic development, angiogenesis, wound healing, nerve regeneration, chronic inflammation and cancer (Ornitz & Itoh, 2015). Till date 22 members have been identified (FGF-1 to 14 and FGF-16 to 23) (Itoh, 2007). These are further sub-divided into six sub-families. FGFs modulate proliferation and differentiation of a variety of mesenchymal and neuroectodermal cells (Bellosta et al., 2001) . They also play critical roles during numerous embryonic process including mesoderm induction, limb and lung development and blastocyst development (Bellosta et al., 2001). According to literature, a number of human skeletal

disorders, for instance, dwarfism result as a consequence of increased FGF signaling (Bellosta et al., 2001). The major role of FGFs is in wound healing and physiological and pathological angiogenesis (Bellosta et al., 2001).

FGFs, in contrast to other growth factors bind heparin or extracellular heparin sulfate proteoglycan (HSPG) to activate FGFRs and have a homologous central core of 140 amino acids (Woodbury & Ikezu, 2014).

1. HS and HSGAGs

Extracellular complex polysaccharides such as heparin, heparin sulfate (HS) and heparan sulfate glucosaminoglycans (HSGAGs) have important roles in developmental biology and cancer biology (Raman et al., 2003). These HSGAGs bind morphogens, growth factors and enzymes in a sequence-specific manner and result in influencing the physiological state of cells and tissues (Raman et al., 2003). They are necessary components for growth factor binding to its receptors leading to a biological response: development, inflammation, immune response and disease (Bellosta et al., 2001). Therefore, it is essential to understand how HSGAG-protein sequence-specific interactions result in important signaling cascades such as FGF-FGFR signaling (Raman et al., 2003). HSGAG regulates FGF signaling differentially via the cell surface tyrosine kinase receptors (FGFR).

HS is essential for the normal functioning of a number of developmental pathways including: FGF, Wingless/Wnt, Dpp (decapentaplegic)/BMP (bone morphogenetic protein) and Hedgehog as revealed by genetic studies carried out in different model organisms including *Drosophila* (Kreuger et al., 2005). Enzymes involved in HS biosynthesis result in abnormal distribution and signaling of these growth factors and morphogens if defective/mutated (Kreuger et al., 2005).

HSGAGs as shown in Figure A1 mediate FGF binding to FGFRs, generating a ternary complex that is required for downstream signaling (Venkataraman, Shriver, Davis, & Sasisekharan, 1999). FGFs interact with the sulfated domains of heparin sulfates (HS) moieties of cell surface and extracellular matrix-associated heparan sulfate proteoglycans (HSPGs) (Ostrovsky et al., 2002). They also interact with heparin, which is a highly sulfated polysaccharide that shares structural similarity with heparan sulfates and can therefore mimic their action (Ostrovsky et al., 2002). These molecules protect FGFs from heat inactivation and proteolytic degradation and provide an extracellular reservoir from which FGFs can be rapidly released (Ostrovsky et al., 2002).

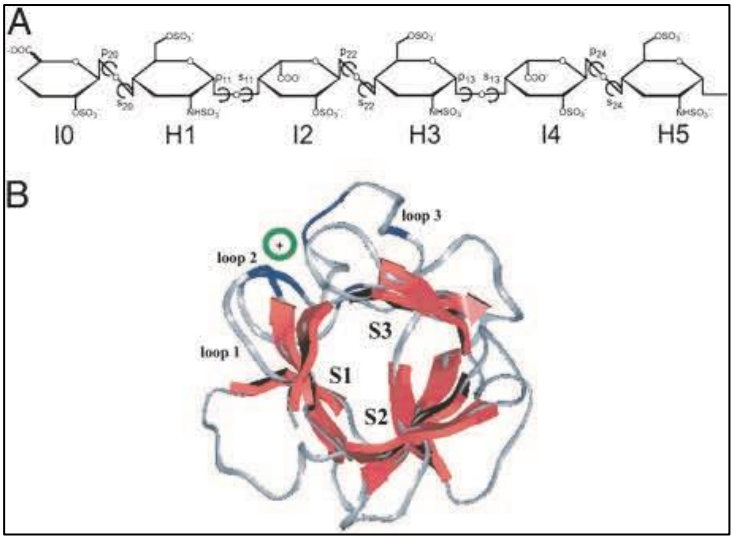

Figure A1. FGF-HSGAG structural complex. (A) HSGAG oligosaccharide chemical structure. (B) β-trefoil scaffold of FGF and the orientation of HSGAG oligosaccharide as shown by dotted-green circle. (Raman, Venkataraman, Ernst, Sasisekharan, & Sasisekharan, 2003)

According to the Figure A1, HSGAGs are linear polysaccharides, which are characterized by a disaccharide repeat unit of a-D-glucosamine (1→4) linked to pyranosyluronic acid (Muñoz & Linhardt, 2004; Raman et al., 2003). An acetyl or sulfo group may be substituted

at the amino group of the glucosamine residue (Raman et al., 2003). HS, like HSGAG is also a linear copolymer of uronic acid 1→4 linked to glucosamine, but unlike HSGAG has a more varied structure and is less substituted in sulfo groups than heparin (Kreuger et al., 2005; Muñoz & Linhardt, 2004). D-glucuronic acid predominates in HS, although substantial amounts of L-iduronic acid can be present (Muñoz & Linhardt, 2004). The glucuronic acid composed precursor HS is modified partially through a series of reactions involving N-deacetylation and N-sulfation, etc (Kreuger et al., 2005). These reactions are variably regulated in different cells and tissues and also at different developmental stages, therefore, the modified mature HS is shown to contain sulfated domains of variable length and composition (Esko & Lindahl, 2001; Gallagher, 2001). These domains are important because they provide binding sites for protein ligands (Kreuger et al., 2005).

The interactions between FGF and HSGAG are predominantly ionic, with van der Waal forces also influencing the FGF-HSGAG binding (Raman et al., 2003). Upon FGF binding, a kink is introduced in the helix axis of HSGAG (Raman et al., 2003). In addition, the spatial distribution of basic residues in the protein is another structural feature that facilitate interaction between HSGAG and FGF (Raman et al., 2003). These basic residues interact with the sulfate groups in the interacting HSGAG chain (Raman et al., 2003). The FGF-HSGAG structural complex is shown in Figure A1.

Figure A1 (B) shows the β-trefoil scaffold of FGF and the orientation and chain direction of the HSGAG oligosaccharide relative to the sheets shown (S1, S2, and S3). The dark blue regions in the loops represent the basic residues that the oligosaccharides (shown by the green circle) interact with (Raman et al., 2003).

FGF members bound to heparin have been shown to exhibit increased stability in the

presence of acid, heat, mild oxidation, and proteolysis (DiGabriele et al., 1998) . This is significant, since human FGF1, in the absence of sugar poly anions, tends to unfold at physiological temperature (Blaber, DiSalvo, & Thomas, 1996; Yeh et al., 2002).

2. Heparin and Heparin-binding pocket

Heparin is the most widely used anticoagulant (Muñoz & Linhardt, 2004). Heparin is primarily intracellular, whereas HSGAG are common components of cell surface and extracellular matrix (Muñoz & Linhardt, 2004). Heparin binds to numerous proteins including proteases, growth factors, chemokines, lipid-binding proteins and pathogen proteins (Muñoz & Linhardt, 2004).

Heparin is negatively charged due to sulfo and carboxyl groups present in the disaccharide (Muñoz & Linhardt, 2004). This is why the interaction of heparin with other proteins is ionic in nature. The heparin-binding pockets in proteins are characterized by the presence of positively charged amino acids (Muñoz & Linhardt, 2004). Hydrogen bonding and hydrophobic interactions also contribute to the stability of heparin-protein complexes (Muñoz & Linhardt, 2004). The interaction of heparin and protein is sequence-specific (Muñoz & Linhardt, 2004). A consensus sequence exists in the heparin-binding pocket of proteins that is necessary for the generation of heparin-protein complex with appropriate affinity and specificity (Blaber et al., 1996; Muñoz & Linhardt, 2004).

The most frequent residues present in the heparin- and heparan sulfate (HS)-binding proteins are arginine and lysine (Muñoz & Linhardt, 2004). Arginines bind more tightly as compared to lysines, even though both carry a positive charge at physiological pH. This is because arginine forms stable hydrogen bonds and stronger electrostatic interactions with sulfo groups present in heparin and HS (Muñoz & Linhardt, 2004). Serine and glycine are some non-

basic residues that are also known to play a role in heparin-protein interactions because their smaller side-chains, thereby providing more flexibility and less steric constraints (Muñoz & Linhardt, 2004).

In order to determine the critical amino acids and their spatial arrangement in heparin-binding proteins like FGF and to identify the consensus sequence present in heparin-binding pocket of heparin-binding proteins, the 3D protein structure and the structure of heparin-binding site needs to be established. This can be done through X-ray crystallography, which provides high-resolution structural information about the protein complexes. The structure of heparin in complex with fibroblast growth factors (FGFs) is present (Muñoz & Linhardt, 2004). The analysis of the heparin-protein complex can reveal the residues present in the heparin-binding pocket by the proximity of basic amino acids to negatively charged groups in heparin. In order to determine the significance of each residue involved in binding, side-directed mutagenesis of the wild-type protein can be carried out. Detailed characterization of heparin-binding sites on proteins can be obtained by carrying out binding studies and biological activity assays. Affinity chromatography is one the most commonly used techniques to study the binding affinity of heparin-protein interactions (Muñoz & Linhardt, 2004). Understanding the interactions of heparin with proteins at the molecular level will help in improved understanding of designing therapeutic drugs that can be employed in disease and pathology.

A specific region of FGF molecule interacts with FGF receptors and heparin (Ornitz & Itoh, 2001). The receptor-binding site is contiguous with the heparin-binding site. This region is located at loop 3/hairpin 3 segment of human acidic FGF (FGF-1) (Ornitz & Itoh, 2001). This region is used commonly as a model for the design of peptide-based agonists/antagonists of the FGFs (Ornitz & Itoh, 2001).

3. Heparin-binding Domains of FGF1

Heparin potentiates the mitogenic activity of FGF-1 and protects it from proteolysis (trypsin digestion) and heat inactivation (Wong et al., 1995). Binding to heparin increases FGF stability under oxidizing conditions (low pH and higher temperatures) (Pineda-Lucena et al., 1994). It also increases the apparent affinity of FGF-1 for FGFRs (Wong et al., 1995). Identification of the heparin-binding domain of FGF1 was therefore significant and aided in the development of peptide-based antagonists of its function (Wong et al., 1995).

A number of consensus sequences of the heparin-binding regions in heparin-binding proteins were proposed and included the motifs XBBXBX and XBBBXXBX, where B and X are basic amino acid and hydropathic residue, respectively (Wong et al., 1995). FGF1 amino acid sequence was analyzed and it revealed the presence of three regions including residues 22-27, 113-120 and 124-131 that is in agreement with the proposed consensus sequences (Wong et al., 1995). The affinity of recombinant FGF1 for heparin is reduced when lysine 132 in FGF1 is mutated to a glutamic acid (K132E) or glycine (K132G) by side-directed mutagenesis, even though lysine 132 lies outside the regions of FGF1 residues proposed (Wong et al., 1995). This was determined using affinity chromatography. The mutant still binds and activates FGFRs and transcribes a variety of immediate-early genes (Wong et al., 1995). Changing lysine 23, 24, or 26 to glycine does not alter the affinity of the mutants to heparin binding, whereas there was minor reduction when residues 113-120 were modified (Wong et al., 1995). On the other hand, mutating residues in the third proposed region 124-131 had significant and varying effects on heparin binding (Wong et al., 1995). The reduction in the binding affinities of most of the mutant proteins (124-131) was mostly due to change in mutants protein folding and stability (Wong et al., 1995). The binding affinities were observed in the presence of exogenous heparin, so that

binding to cell surface HSPGs was inhibited (Wong et al., 1995).

A more stringent analysis of the heparin-binding pocket of FGF1 revealed that basic residues 126 and 133 are crucial to heparin binding (Wong et al., 1995). These residues satisfied the spatial requirement of basic amino acids at opposite ends of a beta-strand fold (Wong et al., 1995).

Mutations in the heparin-binding regions of FGF1 and FGF2 have resulted in reduced mitogenic activities (Mohammadi et al., 2005). Heparin and HS are proposed to not only stabilize and protect FGF from heat and proteolysis degradation, they also facilitate the interaction of FGFs with FGFRs by inducing a conformational change in the tertiary structure of FGF and act as storage reservoirs where FGF can be liberated for interaction with FGFR (Mohammadi et al., 2005). Genetic studies in mice and flies have also shown that HS is required for FGF signaling in whole organisms (Mohammadi et al., 2005). Since binding of heparin and heparin sulfates is the primary step in the formation of FGF-FGFR-heparin ternary complex and is absolutely required for FGF signaling; characterizing the heparin-binding region of FGF is necessary and significant.

4. Broad function of FGF

FGFs play an important role in the regulation of proliferation and differentiation in stem cells: embryonic stem cells, Trophoblast stem cells and neural stem cells. They also play important roles in development and morphogenesis (Venkataraman et al., 1999). Members of the FGF family function in the earliest stages of embryonic development and also during organogenesis in order to maintain progenitor cells and mediate their growth, differentiation, survival and patterning (Ornitz & Itoh, 2015). In adult tissues FGFs are involved in the mediation of metabolic functions, tissue repair, regeneration, and also reactivate some

developmental signaling pathways (Ornitz & Itoh, 2015). They are also involved in tissue repair and activate appropriate signaling pathways in response to injury (Ornitz & Itoh, 2015).

The regulation of differentiation of the inner mass cells (IMCs) into the epiblast and primitive endoderm lineages in regulated by FGFs during early development (Ornitz & Itoh, 2015). During later developmental stages, FGFs are involved in organogenesis, which includes the regulation of anterior and secondary heart fields, induction of limb and lung buds, liver, pancreas, kidney and brain development (Ornitz & Itoh, 2015).

5. FGF-Receptor- The Chemistry and Structure

The various biological processes regulated by FGFs require spatial and temporal integration of several cell responses, including cell survival, proliferation, migration and invasion, and cell differentiation (Bellosta et al., 2001). These diverse effects of FGFs are mediated by four tyrosine kinase receptors of ~800 amino acids, FGF receptors (FGFR-1 to 4) (Bellosta et al., 2001). Fibroblast growth factor receptors (FGFRs) are located on cell surface membranes (Kan et al., 1996).

Figure A2 represents the FGFR protein structure (Ornitz & Itoh, 2015). The figure also represents the splice variants of FGFR proteins. FGFR1-3 generate two splice variants of Ig-like domain III, (IIIb and IIIc) (Ornitz & Itoh, 2015). These major variants are essential ligand-binding specificity determinants (Ornitz & Itoh, 2015).

The tyrosine kinase domain located in the cytoplasmic part. The cytoplasmic domain also contains extra regulatory sequences (Ornitz & Itoh, 2015). These receptors share common features, which include an extracellular ligand-binding domain, a transmembrane domain and a conserved cytoplasmic tyrosine kinase domain (Bellosta et al., 2001; Bikfalvi, Klein, Pintucci, & Rifkin, 1997; Ornitz & Itoh, 2015). The extracellular ligand-binding domain contains

immunoglobulin-like domains D1-D3 (Bellosta et al., 2001; Bikfalvi et al., 1997). Several isoforms of FGFRs exist because of alternating splicing of D1-D3 immunoglobulin domains of RTKs as shown in Figure (Ornitz & Itoh, 2015). There is an acid box region containing 7-8 acidic residues in between D1 and D2 (Bellosta et al., 2001; Ornitz & Itoh, 2015). The ligand-binding domain is located specifically between D2 and D3 and the short D2-D3 linker (Bellosta et al., 2001).

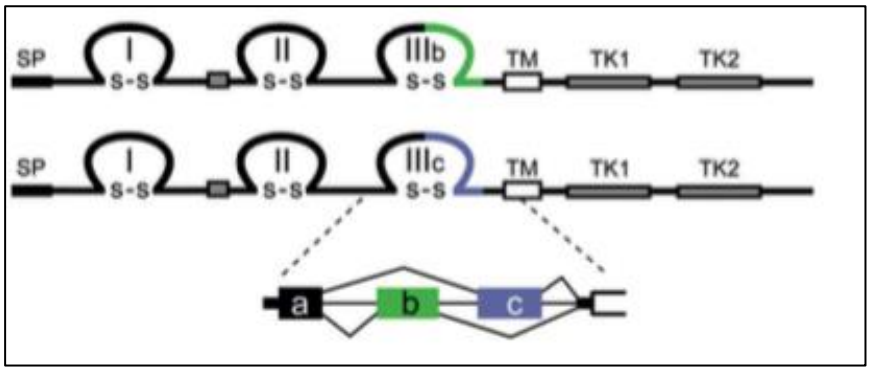

Figure A2. Schematic representations of FGFR protein structures. The figure represents three extracellular immunoglobulin-like domains (I, II, and III), a transmembrane domain (TM), and two intracellular tyrosine kinase domains (TK1 and TK2). SP-cleavable secreted signal sequence. (Ornitz & Itoh, 2015)

The FGFR receptor families are conserved in humans, *Drosophila, C. elegans*, etc (Bikfalvi et al., 1997). Mutations in the FGFR can lead to abnormal morphogenesis, and the progression of several types of cancers (Ornitz & Itoh, 2015).

6. <u>Classification of each form of FGF</u>

The fibroblast growth factor family presently has 23 members (Ornitz & Itoh, 2015). Each of these members has HSGAG-binding domain that varies from member to member (Raman et al., 2003). The members of the FGF family can be found in different organisms from nematodes to humans (Belov & Mohammadi, 2013). Homology and phylogenetic studies reveal

that these members are grouped into seven sub-families as shown in Figure A3 (Ornitz & Itoh, 2015).

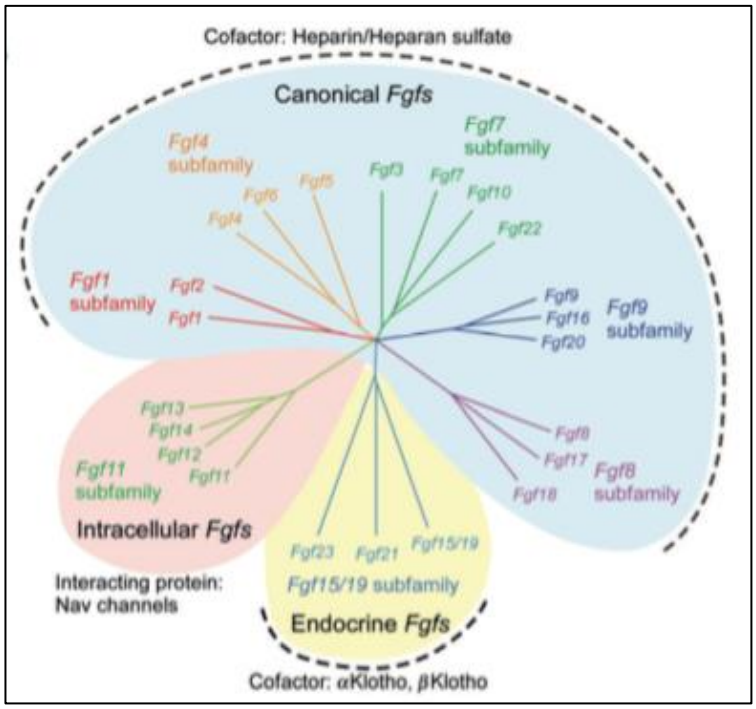

Figure A3. FGF families. According to phylogenetic analysis, 22 members of FGF are categorized in seven subfamilies. The branch lengths represented in this figure are proportional to the evolutionary distance between each gene member. (Ornitz & Itoh, 2015)

The families are characterized based on their function, sequence similarity and mode of signaling (Belov & Mohammadi, 2013). Members of the FGF family are related by core sequence and structure conservation and are found in both vertebrates and invertebrates (Ornitz & Itoh, 2015). The first five subfamilies are involved in paracrine signaling (acts locally) and the sixth subfamily (FGF19, 21 and 23) is involved in endocrine signaling (long-distance) (Pellegrini et al., 2000). In general, secreted FGFs function as autocrine or paracrine factors (canonical FGFs), whereas FGF19, 21 and 23 (three members of the secreted FGFs) have evolved to function as endocrine factors (Ornitz & Itoh, 2015). Endocrine FGFs regulate

phosphate, bile acid, carbohydrate and lipid metabolism in adults, whereas paracrine FGFs control cell proliferation, differentiation and survival (Ornitz & Itoh, 2015).

The human FGF genes are expressed at different unique sites and are expressed differentially in tissues (Ornitz & Itoh, 2015). For instance, FGF 3, 4, 8, 15, 17, and 19 are expressed during embryonic development (Belov & Mohammadi, 2013). FGF 1, 2, 5, 6, 7, 9-14, 16, 18, 20-23 are expressed in embryonic and adult tissues (Belov & Mohammadi, 2013). Except FGF16, the gene locations of all 22 FGF genes are known. The gene locations are various for all human FGF genes; they are created through chromosomal events such as translocation and chromosomal duplication (Belov & Mohammadi, 2013).

Seven FGF subfamilies as represented in Figure A3 ((Ornitz & Itoh, 2015).

I. FGF1 Subfamily (FGF1 and FGF2)

FGF1 and FGF2 belong to FGF1 subfamily and lack classical secretory signal peptides (Ornitz & Itoh, 2015). However, they can be exported out from the cells directly by translocation across the cell membrane (Ornitz & Itoh, 2015). A chaperone complex that includes synaptotagmin-1 and calcium-binding protein (S100A13) is involved in translocation (Ornitz & Itoh, 2015). Both FGF1 and FGF2 have also been found in the nucleus (Ornitz & Itoh, 2015).

a. Acidic FGF (FGF1)

Human acidic FGF (FGF1) is a 16-kDa polypeptide, which was purified from brain originally (Pineda-Lucena et al., 1994). The crystal structure of FGF1 reveals that it consists of twelve antiparallel B strands (Pellegrini et al., 2000). Six beta-strand pairs within the beta-trefoil fold at the base of three of the strand pairs create a beta-barrel (Pellegrini et al., 2000). In addition, five of the pairs are designed as a hairpin structure (Pellegrini et al., 2000).

b. Basic FGF (FGF2)

Human Basic FGF (FGF2) has pleiotropic effects in different tissues and organs, and has a role in angiogenesis, differentiation and the function of the central nervous system (CNS) (Bikfalvi et al., 1997; Woodbury & Ikezu, 2014). Five different polypeptides can be formed from the same FGF2 gene via five different mRNA translation initiation sites (Woodbury & Ikezu, 2014). FGF2 is an established neurogenic factor for proliferation and differentiation of multipotent neural stem cells during development (Bikfalvi et al., 1997; Woodbury & Ikezu, 2014). It is also a potent angiogenic molecule, which is known to stimulate smooth muscle growth, wound healing and tissue repair *in vitro* as well as *in vivo* (Bikfalvi et al., 1997).

FGF-2 was initially isolated from pituitary gland and was identified as a 146-amino acid protein (Bikfalvi et al., 1997; Pineda-Lucena et al., 1994). It is closely related (55% similarity) to FGF1 (Pineda-Lucena et al., 1994).

The structure of FGF-2 reveals the presence of 12 anti-parallel beta-sheets, which are organized into a trigonal pyramidal structure (Bikfalvi et al., 1997). The receptor-binding sites are located between the residues 13-30 and 106-129 (Bikfalvi et al., 1997).

II. FGF4 Subfamily (FGF4, FGF5, FGF6)

Members of the FGF4 subfamily are secreted proteins and have cleavable N-terminal signal peptides (Ornitz & Itoh, 2015). FGF4, unlike FGF1 and FGF2 has a classical signal peptide and is secreted from cells efficiently (Bellosta et al., 2001). Members of this subfamily activate IIIc splice variants of FGFRs 1-3 as shown in Figure A2 and FGFR4 (Ornitz & Itoh, 2015).

III. FGF7 Subfamily (FGF3, FGF7, FGF10, FGF22)

Members of this subfamily of proteins activate the IIIb splice variant of FGFR2, preferentially (Ornitz & Itoh, 2015). FGF3 and FGF10 are also known to activate the IIIb splice variant of FGFR1 (Ornitz & Itoh, 2015).

IV. FGF8 Subfamily (FGF8, FGF17, FGF18)

Members of this family, like the FGF4 subfamily also contain an N-terminal cleavable signal peptide and activate IIIc splice variants of FGFRs 1-3 and FGFR4 (Ornitz & Itoh, 2015).

V. FGF9 Subfamily (FGF9, FGF16, FGF20)

FGF9, 16 and 20 do not have an N-terminal cleavable signal peptide, but they have an internal hydrophobic sequence (Ornitz & Itoh, 2015). This sequence facilitates in the transport of these FGFs into the endoplasmic reticulum (ER) and secretion from cells (Ornitz & Itoh, 2015). They also activate the IIIc splice variants of FGFRs 1-3 and FGFR 2, like members of FGF4 and FGF8 subfamily, in addition to IIIb splice variant of FGFR3 (Ornitz & Itoh, 2015).

VI. FGF15/19 Subfamily (FGF19, FGF21, FGF23)

FGF-19 subfamily members include FGF-19 (the human ortholog of mouse FGF-15), FGF-21 and FGF-23 (Pellegrini et al., 2000). Members of this subfamily are endocrine FGFs (Ornitz & Itoh, 2015). The affinity of these FGFs to heparin is weak, and therefore require cofactors; members of the Klotho family, for receptor binding and subsequent activation (Ornitz & Itoh, 2015). This aids in the release of FGFs from ECMs (Ornitz & Itoh, 2015).

VII. FGF11 Subfamily (FGF11-14)

FGF 11-14 are intracellular FGFs (Ornitz & Itoh, 2015). FGF-11 to 14 are members of the FGF-11 subfamily and are also known as fibroblast growth factor-homologous factors (FHFs). They have high sequence and structural homology with FGFs and bind HSPG with high affinity.

Generally, they are not considered as members of the FGF family. This is because they do not activate FGFRs, most likely due to structural incompatibility of the FGFR-interacting region. FHFs act as intracellular signaling molecules via interaction with islet brain-2 scaffold protein and cytoplasmic carboxy terminal tail of voltage-gated sodium channels (Ornitz & Itoh, 2015).

The receptor specificity of all subfamilies of FGFs for FGFRs is summarized in the Table A1.

FGF subfamily	FGF	Cofactor	Receptor specificity
FGF1 subfamily	FGF1		All FGFRs
	FGF2		FGFR 1c, 3c > 2c, 1b, 4Δ
FGF4 subfamily	FGF4		FGFR 1c, 2c > 3c, 4Δ
	FGF5		
	FGF6		
FGF7 subfamily	FGF3	+ Heparin or Heparan sulfate	FGFR 2b > 1b
	FGF7		
	FGF10		
	FGF22		
FGF8 subfamily	FGF8		FGFR 3c > 4Δ > 2c > 1c >> 3b
	FGF17		
	FGF18		
FGF9 subfamily	FGF9		FGFR 3c > 2c > 1c, 3b >> 4Δ
	FGF16		
	FGF20		
FGF15/19 subfamily	FGF15/19	+βKlotho	FGFR 1c, 2c, 3c, 4Δ
	FGF21		FGFR 1c, 3c
	FGF23	+αKlotho	FGFR 1c, 3c, 4

Table A1. Receptor specificity of canonical and endocrine FGFs. Table adapted from (Ornitz & Itoh, 2015).

7. FGF Signaling process

The binding of FGF and HSPG to the extracellular ligand domain of FGFR induces receptor dimerization, activation and auto-phosphorylation of multiple tyrosine residues in the cytoplasmic domain of the receptor molecule (Mohammadi et al., 2005). When FGF-heparin complex binds to the D2-D3 region of the FGFR, the receptor dimerizes. This leads to auto-phosphorylation of seven tyrosines in the protein tyrosine kinase (PTK) domain of the FGFR,

activating various signaling pathways that include RAS-MAPK, PI3K-AKT, PLC-gamma, and STAT intracellular signaling pathway (Ornitz & Itoh, 2015).

FGFR binding specificity is an essential mechanism in the regulation of FGF signaling. Autocrine or paracrine FGFs, also known as canonical FGFs are tightly bound to heparin/ heparan sulfate (HS) proteoglycans (HSPGs), which tightly regulate the FGF-FGFR signaling pathway by limiting the diffusion through the extracellular matrix (ECM) and also by serving as cofactors, thereby regulating the specificity and affinity of FGFs for FGFRs (Ornitz & Itoh, 2015).

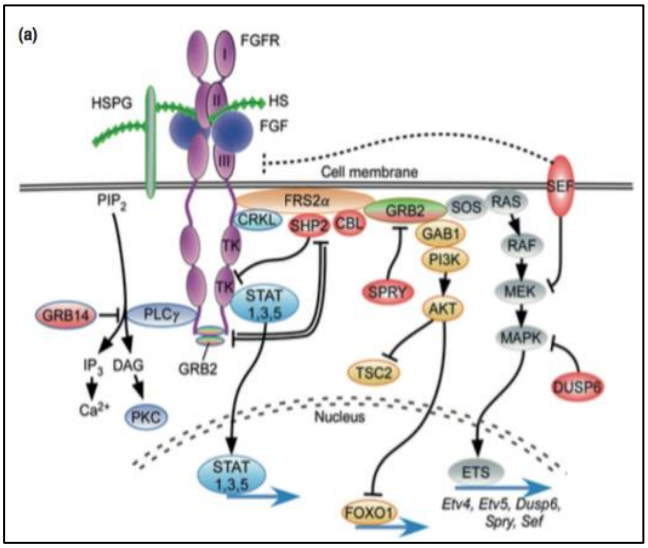

Figure A4. FGF Signaling Pathways. Figure adapted from (Ornitz & Itoh, 2015).

Binding of FGF to FGFR tyrosine kinase results in the sequential phosphorylation of six tyrosine residues, the phosphorylation of all is required for the full activation of the kinase domain (Ornitz & Itoh, 2015). Y653 is initially phosphorylated, which results in a 50-100-fold increase in the tyrosine kinase activity (Ornitz & Itoh, 2015). This is followed by Y583, Y463, Y766 and Y585 phosphorylation in that order (Ornitz & Itoh, 2015). In the third and last phase of receptor activation, Y654 is phosphorylated, which causes a further ten-fold (500-1000-fold)

increase in the activation of the receptor (Muñoz & Linhardt, 2004). Four major intracellular signaling pathways are then activated by tyrosine kinase FGFR activation: RAS-MAPK, PI3K-AKT, PLC-gamma, and signal transducer and activator of transcription (STAT) as shown in Figure A4 (Ornitz & Itoh, 2015). Activation of PLC-gamma and STAT3, however requires the phosphorylation of two additional tyrosine residues Y677 and Y766 (Ornitz & Itoh, 2015).

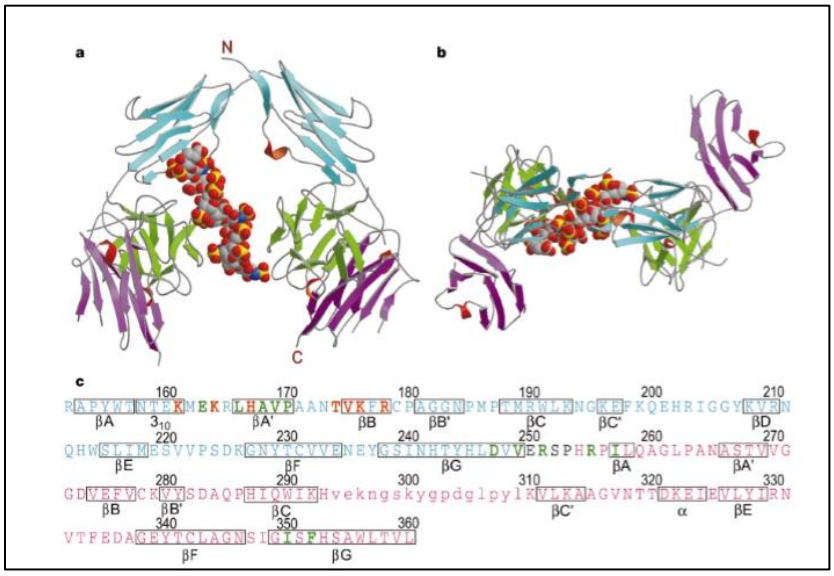

Figure A5. FGF1-FGFR2-Heparin Complex. (a) D2 and D3 domains of FGFR2 shown in cyan and magenta, respectively. FGF1 is green. Heparin molecule is shown in the middle in CPK representation. (b) Different representation. (c) Ligand-binding region of human FGFR2 with cyan and magenta regions representing D2 and D3. Boxed regions are secondary structures. Figure adapted from (Pellegrini et al., 2000)

8. FGF1-FGFR

FGF1 is a universal ligand for all FGFRs (1-4) (Bellosta et al., 2001). Most of FGF members bind FGFRs promiscuously, although the binding is specific (Bellosta et al., 2001). Crystal structures of FGF1-FGFR1, FGF2-FGFR1 and FGF2-FGFR2 complexes were compared and it was shown that FGF N-terminal (region immediately adjacent and preceding the beta-

trefoil core domain of FGF) and central regions of FGFR D3 interact specifically (Bellosta et al., 2001; Plotnikov, Hubbard, Schlessinger, & Mohammadi, 2000). There is a general binding interface for FGF-FGFR complexes; where FGF makes contacts with D2 of FGFR and D2-D3 linker as shown in Figure A5 (Bellosta et al., 2001; Plotnikov et al., 2000). The crystal structure of FGF1-FGFR2-heparin ternary complex reveals that the heparin molecule links the two FGF ligands into a dimer, which subsequently acts as a bridge between two FGFR2 receptor chains (Bellosta et al., 2001).

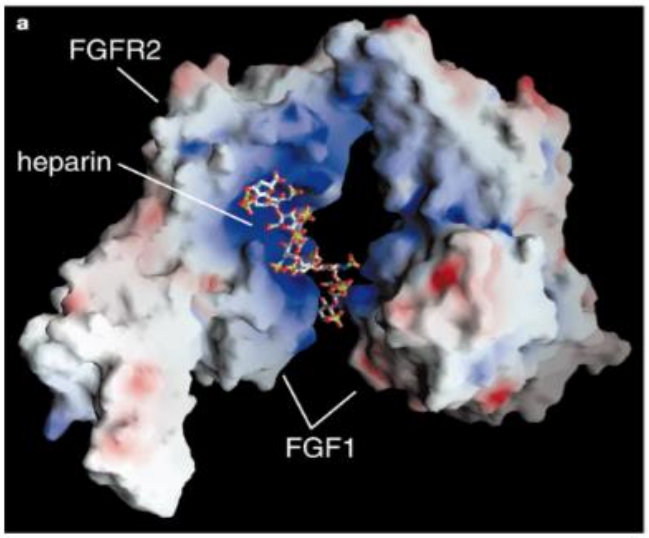

Figure A6. Heparin-binding site in FGF1-FGFR2-heparin ternary complex. Heparin is represented as a stick model. The blue regions in the space-filling model show the positively charged residues that interact with heparin disaccharide. Figure adapted from (Pellegrini, Burke, von Delft, Mullov, & Blundell, 2000).

Literature suggests that heparin plays a dual role in the formation of FGF1 signaling complexes (Gallagher, 2001; Pellegrini et al., 2000). In addition to mediating interaction between FGF1 and FGFR2, it acts as a template for the dimerization of FGF1-FGFR2 subunits (Gallagher, 2001; Pellegrini et al., 2000). This is significant because it can allow the study of heparin-mediated interaction between other ligands and receptors.

The interaction of heparin with FGF1 dimer is shown in Figure A7 generated using Pymol. The interaction of FGF1 with FGFR2 is shown in Figure A8 generated using Pymol.

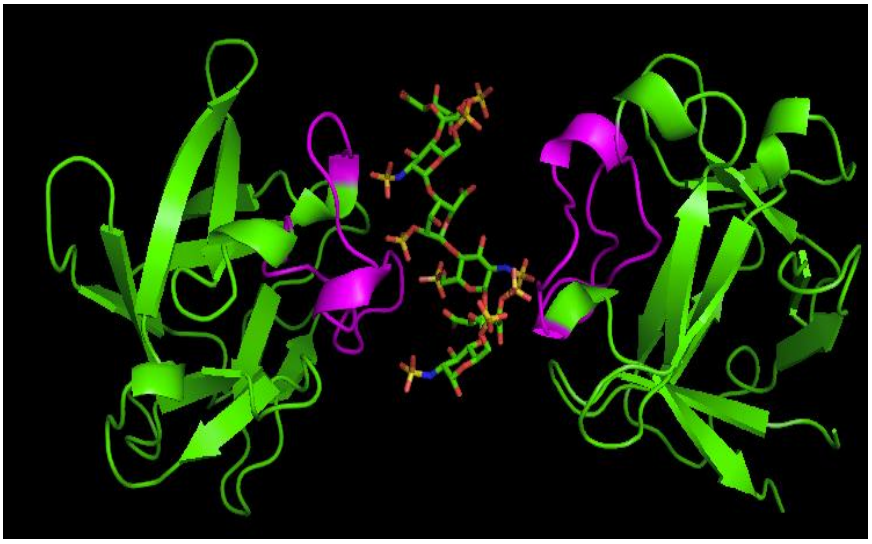

Figure A7. Heparin-linked dimer of Fibroblast Growth Factor 1. Green cartoon model shows FGF1 and the sticks represent heparin. Magenta represents the heparin binding pocket of FGF1 with sequence GSNWFVGLKKNGSCKRGPRTHYGQK: PDB ID: 2AXM. (DiGabriele et al., 1998)

Figure A8. Ligand-binding portion of the Fibroblast Growth Receptor 2 in complex with FGF1. Cyan represents FGFR2 and red represents FGF1, with the heparin-binding pocket of FGF1 represented as magenta. PDB ID: 1DJS. (Stauber, DiGabriele, & Hendrickson, 2000)

9. Application of Basic FGF in medicine

The involvement of FGF signaling in human disease is well documented. Aberrant FGF expression is central to progression of pathogenesis in several disease states, including cancer and chronic inflammation (Venkataraman et al., 1999). Because FGFs are present in almost all adult tissues and organs, consistent with their roles in development and organogenesis, any abnormal activity in the FGF signaling pathway leads to developmental defects that result in the disruption of organogenesis, impair the organism's response to injury, and also result in some metabolic disorders (Ornitz & Itoh, 2015).

10. Rubredoxin (Rub)

Rubredoxin (Rub) is 6.1-kDa red protein that is isolated from *Thermotoga maritime* (Kohli & Ostermeier, 2003). It contains an Fe (III)-cysteine$_4$ center and is commonly used as a colored fusion tag for the expression of recombinant proteins in *E. coli,* like green-fluorescent protein (GFP) and Flavodoxin (Kohli & Ostermeier, 2003). Rub is known to be stable over a wide range of pH, temperature and buffer environments, which facilitates its purification (Kohli & Ostermeier, 2003). It is found in bacteria, archaea and plants (Kohli & Ostermeier, 2003). Most importantly, it provides a direct on-line readout during chromatography; therefore, we employed it in our research project by fusing it to the N-terminal of FGF-peptide.

Rub is a highly soluble bacterial protein and it offers a unique red color, which is directly detectable (Kohli & Ostermeier, 2003). The 3D protein structure of Rubredoxin reveals the presence of the fold that belongs to the +beta class, with 2 -helices and 2-3 beta strands (Kohli & Ostermeier, 2003). The active site of Rub contains an iron ion coordinated by the sulfurs of four conserved cysteine residues, which forms a regular tetrahedron (Kohli & Ostermeier, 2003).

11. Scope of my research

Since many biological processes in humans such as embryonic development, wound healing and angiogenesis require FGF-FGFR signal transduction systems; it is essential to characterize one of the major components of this signal transduction pathways: the characterization of heparin-binding pocket of FGF1 that recognizes the heparin sulfate required for FGF1-FGFR interaction. Characterization of heparin-binding pocket peptide of FGF1 will be useful to design agonists and antagonists for FGF1 which could potentially be used to treat human skeletal disordesrs and block angiogenesis in pathological conditions, for instance, tumor neovascularization.

FGF1 has broad specificity and is unique among all members of the FGF family because it can bind to all seven members of FGF receptor subtypes. Therefore, it is important to characterize the heparin-binding pocket of FGF1 because it is a potent mitogen for various cell types. Understanding the function of heparin-binding peptide in detail can lead to the understanding of FGF1-FGFR interaction and subsequently their roles in diverse biological processes.

B. MATERIALS AND METHODS

1. Competent Cells Preparation

DH5α competent cells were prepared. 50ml of sterile Luria Broth (LB) was inoculated with DH5α from glycerol stocks available in the lab. Media was incubated overnight at 37℃ at 250rpm for 12-16 hours. 500ml autoclaved LB was sub-cultured with 1% primary culture from step 2 and incubated at 37℃ at 250rpm for 2-3 hours. Optical density (OD) was monitored regularly using a spectrophotometer until it reached 0.4-0.5. After the desired OD was reached, the culture was transferred into large volume centrifuge bottles (sterile and pre-chilled) in a sterile laminar hood (250ml/bottle). Centrifugation was carried out at 4500rpm for 15 min at 4℃. The supernatant was discarded aseptically in a sterile laminar hood). To the 250ml harvested cell pellet, 25ml of sterile 0.1M $CaCl_2$ was added and mixed by gently pipetting up and down on ice. The mixture was shifted to sterile and pre-chilled 50ml falcon tubes. Incubation was carried on ice for 15 min. Centrifugation was carried out at 4℃ for 15 min at 4500rpm. Supernatant was then discarded aseptically. 2ml of pre-chilled 0.1M $CaCl_2$ containing 30% Glycerol was added to each of the pellets obtained and cells were delicately mixed by pipetting on ice. The tubes were placed on ice. 100ul of cells were aliquoted in sterile pre-chilled eppendorf tubes and cells were shifted at -80℃.

2. Ampicillin Preparation

50mg/ml stock solution of Ampicillin was prepared by dissolving 0.5g of Ampicillin salt in 10ml ddH_2O and filter sterilized using 0.2 um filter. 1ml aliquots were saved at -20℃. Working concentration of Ampicillin used was 50ug/ml.

3. Isopropyl B-D-1-thiogalactopyranoside (IPTG) Preparation

1M IPTG was prepared by dissolving 1g of IPTG in 5ml distilled, di-ionized water

(ddH_2O) and filter sterilized using 0.2 um filter. Figure B1 shows the structure of IPTG. IPTG activates the lac operon induces protein expression.

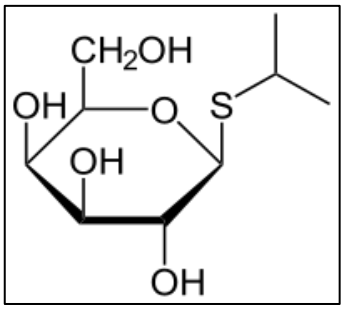

Figure B1. Structure of Isopropyl B-D-1-thiogalactopyranoside (IPTG)

4. **Cloning**

pET22b(+) Vector map and details are in Figure B2. pET22b(+) plasmid was provided. 1ul was transformed into DH5α cells and plated on Agar plates containing 50ug/ml Ampicillin selection. Rub-FGF1-pET22b(+) clone was provided and transformed into DH5α cells and plated on Ampicillin Agar plates. Colonies were picked and plasmid isolation was carried out.

5. **Digestion**

Digestion was set up as shown in Table B1. 50ul digestion mixtures were put in the thermocycler and incubated at 37℃ for 16 hours. 1% agarose gel was prepared in 1X TAE. A preliminary gel was run for the digestion mixtures by loading 4ul of the digested and undigested samples for 30min at 120V in fresh 1X TAE. After confirming that the digestion was complete, the entire remaining digested samples were loaded onto fresh prepared 1% gel and gel run for 40min at 120V.

6. **Antarctic Phosphatase Treatment**

Antarctic phosphatase treatment was carried out for pET22b before the gel for excision

was run, by adding 0.5ul Antarctic phosphatase (AP) enzyme and 5ul AP buffer and sample was incubated in the thermocycler (AP program: 37℃ 15 min and 65℃ 5 min).

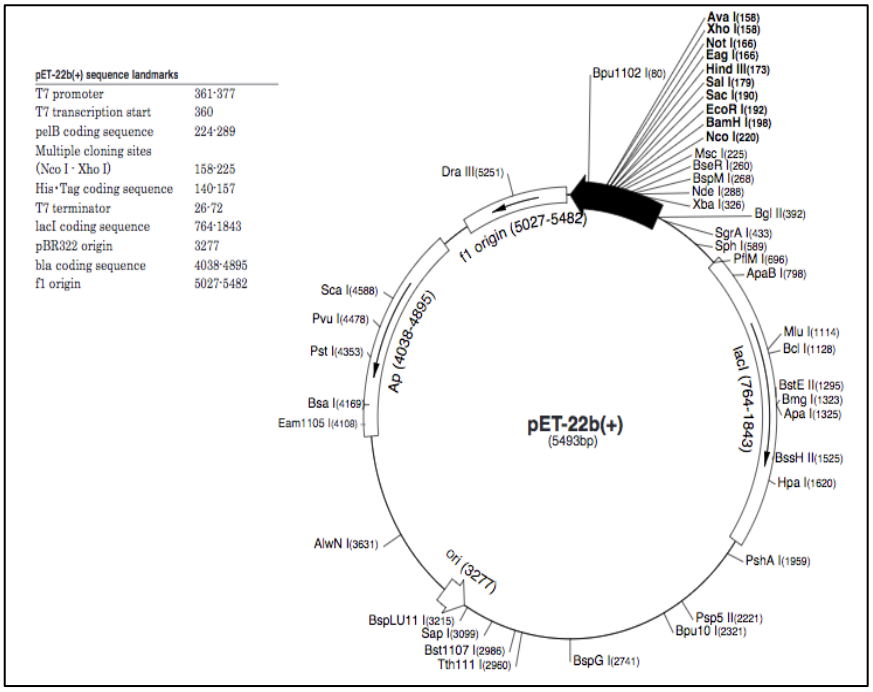

Figure B2. pET22b(+)(+) Vector Map. pET22b(+)(+) was used as a vector for cloning. The gene of interest (Rub-FGF1) was cloned between NdeI and EcoRI sites.

7. Gel Extraction and Elution

Gel excision was carried out under the UV with blade. In case of pET22b(+)-Rub-FGF1 digestion, lower band corresponding to 300bp was excised. The gels were put in respective labeled eppendorfs (weight pre-measured). This step was carried out carefully with minimum UV exposure to the DNA. Gloves were worn at all times when dealing with ethidium bromide. The gel weights were measured. Table B2 shows the respective weights of the gels.

Elution was carried out using QIAgen Gel Extraction Kit. 3 volumes of QG buffer were added to 1 volume of the gel (100mg~100ul). Incubation was carried out at 50℃ for 10 min with vortexing every 2-3 min until the gel completely dissolved. 1gel volume isopropanol was added. The sample was added to QIAquick spin column (in a 2ml collection tube) and centrifugation

was carried out for 3 min at 13000 rpm. Flow through was discarded. 0.75ml PE (Wash Buffer) was added and centrifugation was carried out at 13000rpm for 3min. QIAquick column was placed in a new 1.5ml eppendorf tube. Elution was carried out in 20ul EB (Elution Buffer). 2ul sample of the elution was run and concentration was determined using NanoDrop. The concentrations are as follows:

Rub-FGF1: 14.3ng/ul

pET22b(+): 12.4 ng/ul

Table B1. Digestion

Ingredients	**Vector-pET22b(+)**	**Clone-Rub-FGF1-pET22b(+)**
Cut-Smart Buffer	5ul	5ul
pET22b(+)	42.5ul	-
Rub-FGF1-pET22b(+)	-	42.5ul
EcoRI	1ul	1ul
NdeI	1ul	1ul
BSA	0.5	0.5
MQ-Water	-	-
Total	50ul	50ul

Table B2.

	Empty eppendorf (g)	**Eppendorf + Gel (g)**	**Gel (g)**
pET22b	0.99	1.29	0.03
pET22b-Rub-FGF1	0.99	1.41	0.042

8. Ligation

Ligation was set up as shown in Table B3.

Mixtures were incubated in thermocycler in LIGA program (16℃ overnight).

Table B3. Ligation

	1:3 (ul)	**1:5 (ul)**	**Control (ul)**
Plasmid (pET22b)	3	2	3
Insert (Rub-FGF1)	5	6	-
10X Ligation Buffer	1	1	1
Ligase	1	1	1
ddH_2O	-	-	5
Total	10	10	10

9. Transformation

5ul ligation mixtures were transformed into DH5α competent cells. Incubation was carried out on ice for 15-20min. The cells were heat-shocked at 42℃ for 60 seconds and immediately shifted to ice. 400ul sterile LB media was added and mixtures incubated at 37℃ for 30-45 min. 100ul mixtures were plated on separate labeled Ampicillin Agar plates and incubated overnight (12-14 hours) at 37℃.

10. Plasmid DNA Isolation

5-7ml bacterial culture was inoculated overnight from the colonies in the positive plates. Cells were harvested by centrifugation at 6000rpm for 15 min and supernatant was discarded. The bacterial pellets were re-suspended in 250ul Buffer P1 (Re-suspension buffer containing RNase A) and transferred to a micro-centrifuge tube. 250ul of Buffer P2 (Lysis Buffer) was added and mixed by inverting the tubes 4-6 times. The optimal lysis time is 3-5 min after which the solution gets viscous. 350ul of Buffer N3 (Neutralization Buffer) was added and tubes inverted 4-6 times to ensure mixing. Centrifugation was carried out at 13000rpm for 10min. The supernatant from step 4 was carefully applied to QIAprep spin column by pipette, making sure

not to disturb the pellet. Centrifugation was carried out at 13000rpm for 1min and flow-through was discarded. QIAprep spin column was washed by adding 0.75 ml PE (Wash Buffer) and centrifugation was carried out for 1 min. Flow through was discarded and centrifugation was carried out for an additional minute to remove residual wash buffer. The QIAprep column was placed in a clean 1.5ml microcentrifuge tube. DNA was eluted by adding 25-30ul Buffer EB (10mM Tris.Cl, pH8.5) to the center of the column. The column was left at room temperature for 1-2 min and then centrifugation was carried out for 1 min.

After Plasmid Isolation, digestion was set up using the same enzymes EcoRI and NdeI to confirm successful cloning.

11. Small-Scale Expression (SSE)

Small-scale expression of Rub-FGF1 was performed to verify the absence of fusion protein in BL21 (DE3) cells and ability of these cells to produce the desired protein in the presence of the inducer. 5ml Terrific Broth (TB) was inoculated using glycerol stocks for Rub-FGF1, using 5ul of 50mg/ml Ampicillin selection and incubated at 37C overnight 12-14 hours. This was the primary culture. After 12-14 hours of incubation, 50ml of TB was inoculated with 5ml of the primary culture using 50uL of 50mg/ml Ampicillin and incubated further for 2 hours. Optical density was then checked using UV-visible spectroscopy at a wavelength of 600nm. The blank used was sterile TB. The induction is supposed to be carried out in the log phase, where the bacteria are growing at an exponential rate. The OD at that instant is 0.4-0.6. The OD was 0.547. 1ml sample was saved as Pre-Induced sample to be run on the SDS-PAGE gel.

The secondary culture was then induced using 1M IPTG; 50ul 1M IPTG was added to the culture and cells were incubated for 4 hours at 37C. After four hours, 1ml sample was saved as Post-Induced sample to be run on the SDS-PAGE gel. The cells were then harvested by

centrifuging them for 10 minutes at 6000rpm, 4C and supernatant was discarded. The cells were washed with 1X Phosphate buffer saline (PBS), pH 7.2. The cells were re-suspended in 15ml 1X PBS pH 7.2.

Ultra-sonication was carried out at power 5, 10 pulses on, 10 pulses off for 15 minutes, with 5 min break in-between. This was done to lyse the cells by releasing the cytosol content into the solution. Centrifugation is then carried out at 19000rpm for 30 min at 4C. The cell debris is then separated from the solution that contains the protein of interest. The supernatant, which contains the protein of interest, is transferred to a new falcon. 1ml of supernatant sample is taken to run on the gel. A smear of the pellet is also taken to run the gel.

Samples for SDS-PAGE were prepared. Pre-Induced and Post-Induced samples were centrifuged at 6000 rpm for 5 min and supernatants were discarded.

12. Trichloroacetic acid Precipitation (TCA prep)

100ul of 100% Trichloroacetic acid (10% TCA) was added to 1ml sample of the supernatant saved after high-speed centrifugation. The mixture was vortexed and centrifuged at 13000 rpm for 3 min. Supernatant was discarded. 1ml acetone was added to the pellet and pellet mixed by vortexing. Centrifugation was carried out again at 13000 rpm for 3 min and supernatant discarded again. The sample was air-dried.

To all the four samples: Pre-Induced, Post-Induced, Supernatant and Pellet, 30ul 8M Urea and 15uL Loading dye was added and sample pellets re-suspended. The samples were boiled at 95℃ for 3-5 min and were then loaded onto the SDS gel.

13. Sodium-Dodecyl Sulfate-Polyacrylamide Agarose Gel Electrophoresis (SDS-PAGE)

15% Resolving gel and stacking gel were prepared as shown in Table B4. The gel was run at 200V, 100mA for 50 min. After gel running was complete, the gel was stained in

Coomassie Blue for 3-5 min, gently rinsed with water and put in the de-staining solution overnight with 2 KimWipes overlaid at the top. The gel was scanned the next day.

14. Large-Scale Expression (LSE)

Large-Scale Expression was performed to generate large quantities of Rub-FGF1 protein so that it can be purified for characterization studies. The protocol is exactly similar to SSE, except 150ml of primary culture was inoculated, and 3 liters of secondary culture was inoculated using 25ml of the inoculated and overnight incubated primary culture. Appropriate amounts of 50mg/ml ampicillin and 1M IPTG were added. From the 3 liters culture volumes, 3 falcons containing 1liter pellets were obtained and were saved at -20C. They were dissolved in 25ml 1XPBS pH 7.2 for ultra-sonication and further processing. Samples were collected at each stage to run them on SDS-PAGE.

15. Purification

The pellet obtained from LSE was dissolved in 25 of 1X PBS pH 7.2. Ultra-sonication was performed to lyse the cells and the lysate was separated from the cell debris by centrifugation at 19000 rpm for 30 min at 4C. The supernatant was transferred to a new falcon to be loaded onto the column.

Ni^{+}-NTA column was used for purification since the vector pET22b-Rub-FGF1 has a His-tag at the N-terminal of the protein of interest. The column was pre-equilibrated with 2 column volumes (30ml) of 1X PBS pH 7.2. The supernatant was then loaded onto the column and if peak was observed, then the flow-through was collected. The peak was then base-lined with 1X PBS pH 7.2. 50ml of the following solutions were prepared immediately before they were loaded onto the column and peaks were collected and labeled. The solutions were made up to 50ml with ddH_2O.

Table B4.

	15 % Resolving Gel (2 gels)	**Stacking Gel (2 gels)**
ddH_2O	1.1 ml	3.75 ml
30% Acrylamide	5 ml	0.83 ml
1M Tris.HCl pH 8.8	3.75 ml	-
1M Tris.HCl pH 6.8	-	0.62 ml
10% SDS	100 uL	50 uL
10% APS	100 uL	50 uL
TEMED	10 uL	8 uL

The column was regenerated using two column volumes of 8M Urea (fraction collected), five-column volumes of Milli-Q water and two-columns volumes of 20% ethanol. The column was saved at -20C. TCA precipitation was carried out on 200uL of all the samples collected (flow-through, 20mM, 50mM, 100mM, 250mM and 500mM IMD eluants, 8M urea) and samples were prepared to be run on SDS-PAGE. The purity of the protein was verified by a distinct band at ~10-kDa. The pure protein was collected at 250mM IMD fraction.

16. <u>Concentration and Heat Treatment</u>

The pure protein fraction collected at 250mM IMD was buffer exchanged with 1X PBS pH 7.2 and concentrated using amicon (Millipore centrifugal concentrator) with a 3-kDa molecular weight cut-off. The concentration of the protein was measured using a NanoDrop at 280nm. After concentration, the purified sample was subjected to heat treatment at 75℃ for 10min. The sample was immediately placed on ice. Centrifugation was then carried out at 13K for 3 min. After centrifugation the supernatant was transferred to a new eppendorf. 30ul of the supernatant was prepared for running on the gel. The pellet was also processed for SDS-PAGE. Figure B3 describes the steps used in obtaining compact band.

Table B5.

	4M Imidazole (IMD)	**10X PBS**
20mM IMD	250 uL	5 ml
50mM IMD	625 uL	5 ml
100mM IMD	1250 uL	5 ml
250mM IMD	3250 uL	5 ml
500mM IMD	6250 uL	5 ml

17. Thrombin Cleavage

Depending on the concentration of the heat-treated purified supernatant (determined using NanoDrop at 280nm), thrombin cleavage was set up at room temperature for 1ml of the sample and incubated for 48 hours. After incubation period was over, the sample was heat-treated at 75℃ for 10min and centrifugation was carried out at 13K for 3 min. Supernatant was transferred to new eppendorf and 30ul sample was taken for SDS-PAGE (Sample B). The pellet was also processed (Sample A). 7.5% TCA prep was carried out on the supernatant and the mixture was spun at 13K for 3 min. The supernatant was transferred to fresh eppendorf. The pellet obtained was dissolved in 1ml 1X PBS pH 7.2 and 30ul was taken for SDS-PAGE (Sample C). The supernatant was neutralized using concentrated sodium hydroxide (NaOH) and heat-treated again at 75℃ for 10min. Centrifugation was carried out at 13K for 3 min and supernatant transferred to new eppendorf. Heat-treated pellet post-TCA prep was also processed for running on the gel (Sample D). 30ul of the supernatant was taken for gel too (Sample E). The rest of the supernatant was saved for analysis by mass spectrometry, Circular Dichroism (CD) and Fluorescence.

Samples A-E were processed by adding 30ul 8M Urea and 15ul Loading Dye and boiled at 95℃ for 3-5min. 15ul samples were loaded onto the gel. The flow-chart Figure B4

summarizes the steps followed to obtain the pure FGF1 peptide.

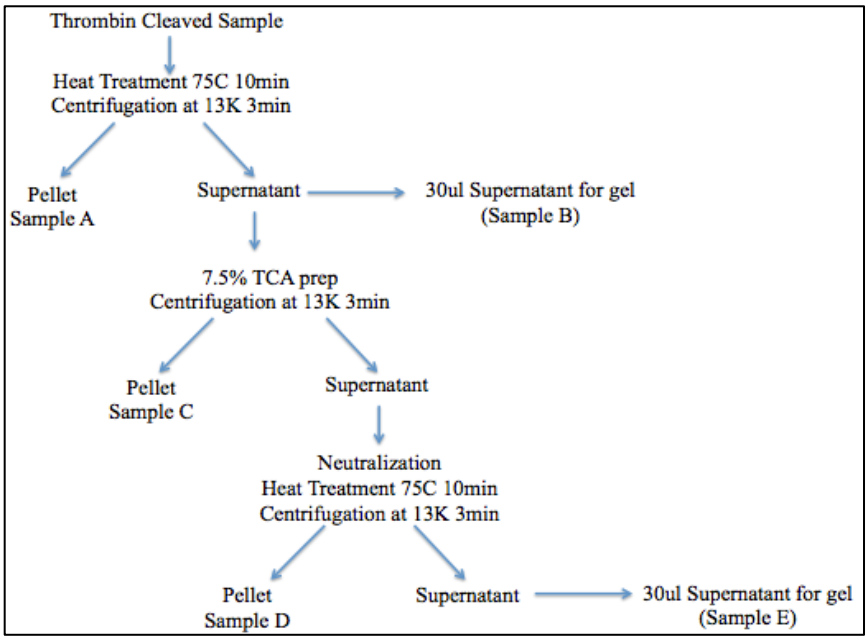

Figure B4. Flow Chart of the Steps followed for the processing of thrombin cleaved sample to obtain pure FGF1 peptide.

18. Far UV Circular Dichroism Spectroscopy

The CD spectra were collected on a Jasco 1500 spectropolarimeter in order to analyze the secondary structure of heparin-binding region of FGF1. A 200ul fraction of the sample was placed in 0.2 cm path length quartz cell. Temperature of the samples was maintained to 25℃. Data were scanned from 190nm to 250nm at a rate of 50nm/min. The scan speed used was 50nm/min and 5 iterations were carried out. Air blank (empty dry cuvette) was done under 300 volts. 1X PBS was used as a blank. The peptide (FGF1) sample was then run. Once the data was collected, it was smoothened using Schvitzky-Golay smoothing algorithm and the buffer signal was subtracted. CD data were transformed into molar ellipticity in the units of degree.cm$_2$/dm of monomer subunits.

19. Intrinsic Fluorescence Spectroscopy

Fluorescence emission spectrum of FGF1 peptide was performed using Hitachi F-2500 spectrofluorometer at 25℃, in a single beam mode. The sample for this experiment was prepared using a protein concentration of 0.87 mg/ml in 1X PBS (pH 7.2). The sample was excited at a wavelength of 280nm, and the data was collected between 300nm and 450nm in order to analyze the fluorescence of tryptophan at 350nm.

20. Mass Spectrometry

20ul of the pure FGF1 peptide obtained by thrombin cleavage was sent to facility in Chemistry/Biochemistry Department. Figure B5 represents the steps involved in obtaining mass spectrum.

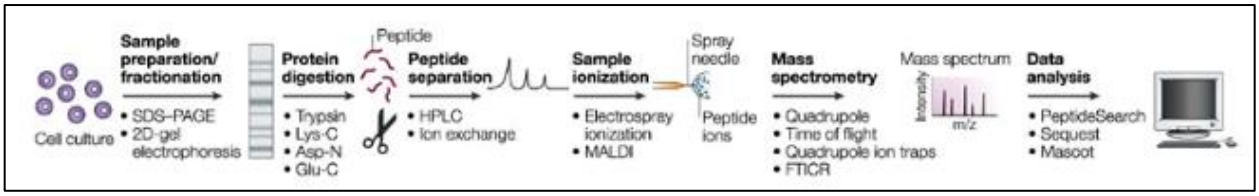

Figure B5. Mass Spectrometry Pipeline. (Steen & Mann, 2004)

Rub-FGF1 was separated by means of an SDS gel and then it was subjected to proteolytic cleavage by thrombin that will result in Rub and FGF1 peptides. The resulting peptides can either be separated by an HPLC or in our case, 7.5% TCA precipitation resulted in pure FGF1 peptide in the supernatant. The peptide was then sent for mass spectrometry. The peptides are ionized before mass spectrometry (Steen & Mann, 2004). The spectrum obtained is then analyzed.

C. RESULTS AND DISCUSSION

1. Cloning of Rub-FGF1

pET22b(+) was used as a vector for cloning. EcoRI and NdeI restriction sites were chosen and the plasmid was digested with these enzymes according to digestion protocol mentioned in materials and methods. pET22b(+) is a 5493bp vector with EcoRI and NdeI restriction sites present at 192bp and 288bp, respectively. Digestion with these two enzymes results in the release of a 96bp band, which is too faint to be observed in a 1% agarose gel. Digestion of pET22b(+) using EcoRI and NdeI is shown in the Figure C1. Digestion results in linearizing pET22b(+) vector generating ~5kb linear plasmid as shown in lanes 2 and 3. Undigested pET22b(+) is shown in lane 1. Since the plasmid is circular, supercoiled and compact, it travels faster as compared to a linear plasmid of the same size and therefore uncut pET22b(+) is observed at ~3-3.5kb. The digested pET22b(+) bands were excised for further experiments.

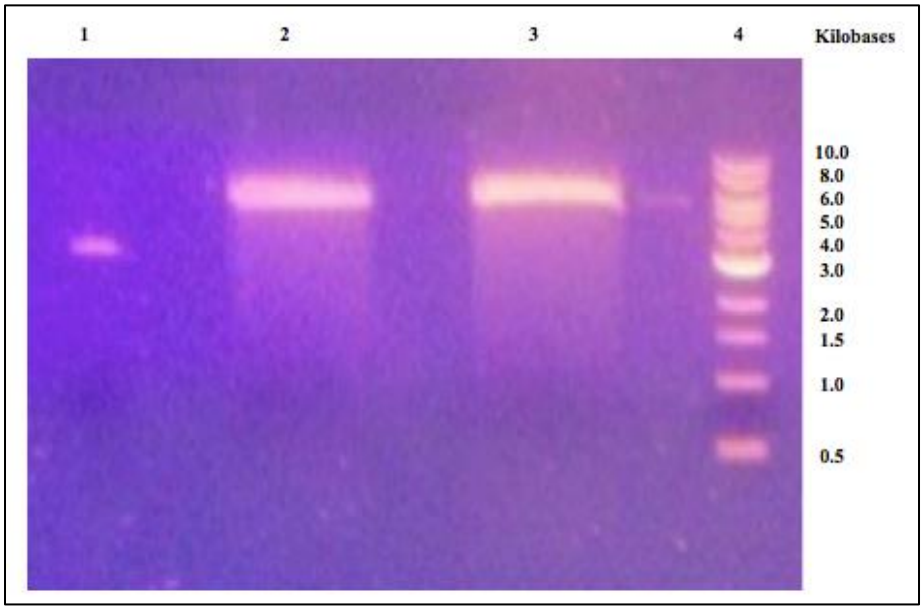

Figure C1. Digestion of pET22b(+) vector using the enzymes EcoRI and NdeI. The lanes correspond to pET22b(+) Uncut (Lane-1), pET22b(+) Cut (Lanes-2 and 3) and 1kb DNA ladder (Lane-4).

Rub-FGF1-pET22b(+) was provided. Rub-FGF1-pET22b(+) is ~5700bp. Digestion of Rub-FGF1-pET22b(+) with EcoRI and NdeI is shown in the Figure C2. After digestion with EcoRI and NdeI, 270bp of Rub-FGF1 is released as shown in Figure C2. The 270bp Rub-FGF1 band was excised for further cloning experiments.

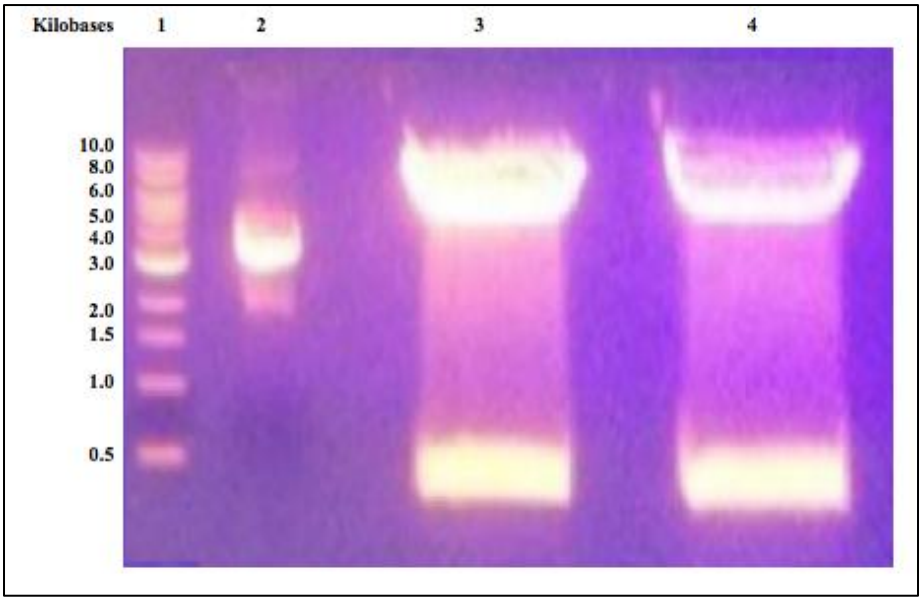

Figure C2. Digestion of Rub-FGF1-pET22b(+) plasmid using the enzymes EcoRI and NdeI. The lanes correspond to 1kb DNA ladder (Lane-1), Plasmid Uncut (Lane-2) and Plasmid Cut (Lanes-3 and 4).

Antarctic phosphatase treatment was carried out for pET22b(+) vector alone before the digestion gels were run. Antarctic phosphatase is thermostable alkaline phosphatase and is purified from a recombinant source. It non-specifically catalyzes the dephosphorylating of the 5' and 3' ends of the DNA sticky phospho-ends generated after digestion. It also acts on the blunt ends generated from some restriction enzymes. It is commonly used in molecular biology and we used to dephosphorylate the vector at both ends to prevent relegation of the linearized pET22b (+) generated after digestion.

The respective gel bands for pET22b(+) Cut and Rub-FGF1 (lower bands) were then excised and gel extraction was carried out using the protocol mentioned in Materials and

Methods section. The elution gel is shown in Figure C3.

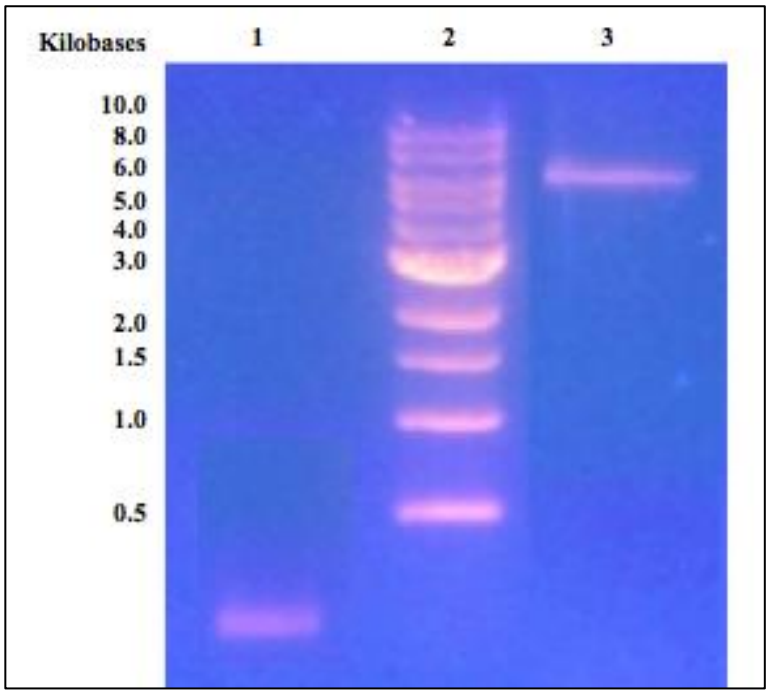

Figure C3. Elution of excised pET22b(+) Cut and Rub-FGF1. The lanes correspond to Rub-FGF1 (Lane-1) and 1kb DNA ladder (Lane-2) and pET22b(+) Cut (Lane-3).

The concentrations were determined, and ligations were set up as mentioned in Materials and Methods. Colonies were observed in both positive 1:3 and 1:5 ligation plates. 2 colonies from both plates were picked and LB was inoculated for plasmid isolation. Digestion confirmation was then carried out with the same enzymes used for initial digestions: EcoRI and NdeI. Figure C4 represents the digestion of 2 plasmids (Rub-FGF1-pET22b(+)). The digestion confirmed that the colonies picked were positive and the plasmid pET22b(+) carried the gene of interest Rub-FGF1, consistent with a 270bp Rub-FGF1 band and ~5300bp Cut pET22b(+) as shown in Figure C4.

2. <u>Small-Scale Expression</u>

Small-scale expression of Rub-FGF1 was carried out after digestion confirmation. The

SDS-PAGE for small-scale expression of Rub-FGF1-pET22b(+) is shown in the Figure C5.

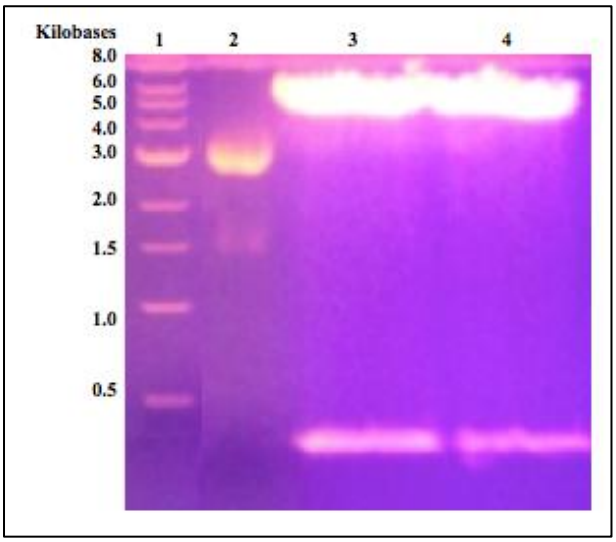

Figure C4. Digestion Confirmation of Rub-FGF1-pET22b(+) plasmid using the enzymes EcoRI and NdeI. The lanes correspond to 1kb DNA ladder (Lane-1), Plasmid Uncut (Lane-2) and Plasmid Cut (Lanes-3 and 4).

Rub-FGF1 is a 90 amino-acids long protein with a size of almost 10kDa. Lane 2 in Figure C5 shows pre-induced sample and has no protein of interest. Lane 3 is the post-induced sample and contains the protein of interest Rub-FGF1. Lane 4 and 5 are pellet and supernatants, respectively obtained after sonication of the cell pellet. Sonication alone was sufficient to get the recombinant protein in the cell lysate and no additional lysis buffers and agents were required. Lane 4 does not contain any protein of interest, which shows that the lysis of the cells was complete. Lane 5 shows the presence of Rub-FGF1 (boxed). This shows that the expression of Rub-FGF1 did take place after cells were induced with IPTG. The same-sized Rub-FGF1 is also present in Lane 3 (post-induced sample). The gel, however, ran a bit slant and therefore the band in this lane appears slightly above than in lane 5.

3. **Purification of Rub-FGF1:**

Figure C6 is the SDS-PAGE analysis of the purification of Rub-FGF1. The expression

and purification of Rub-FGF1 was observed at both 100mM IMD and 250mM IMD with thick compact bands observed at around 10-kDa, consistent with the size of the fusion protein Rub-FGF1 (9.9-kDa).

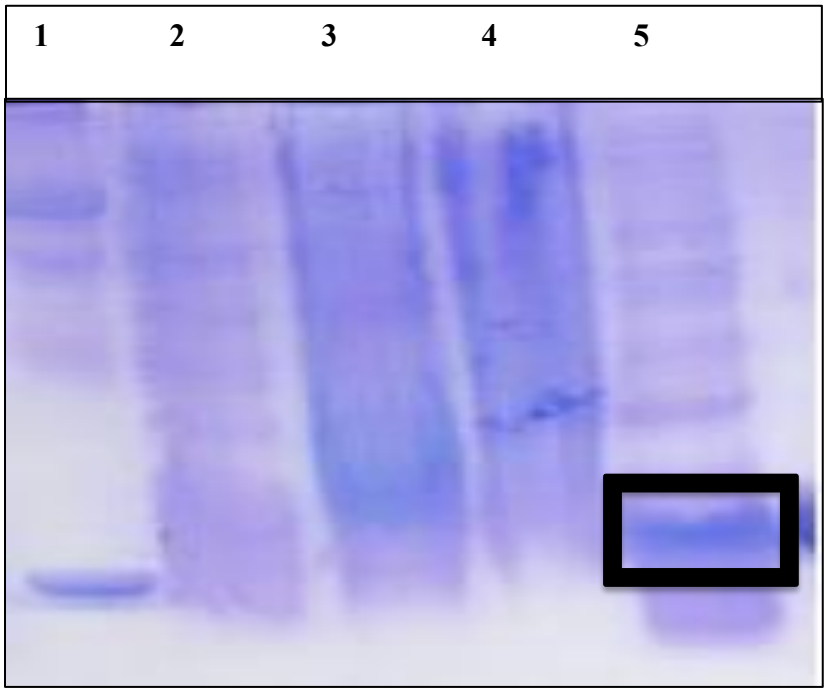

Figure C5. Small-scale expression of Rub-FGF1-pET22b(+) in BL21 (DE3) cells. The lanes correspond to In-house Protein marker (Lane-1), Pre-Induced (Lane-2), Post-Induced (Lane-2), Pellet (Lane-4) and Supernatant (Lane-5).

Ni^{+}-NTA column was used for purification. pET22b(+) has a Histidine tag coding sequence from 140-157bp in the vector as shown in Figure B2. The poly-histidine tag generates a string of histidine residues (6-10) either at the N-terminus or the C-terminus of the recombinant protein after induction with IPTG; in this case it generates hexa-histidine tag located at the N-term of the recombinant protein.

This purification technique is an example of immobilized metal affinity chromatography. The Histidines bind to the Nickel in the column. Nickel is the transition metal that is immobilized on the resin matrix. Cobalt, copper and zinc are examples of other transition metal

ions used for his-tagged recombinant protein purifications. Nickel is most commonly used because it gives high yield. His-tags gave a high affinity for nickel ions and bind to the matrix tightly. The other proteins that are present in the cell lysate either bind weakly to the column or do not bind at all. This way pure recombinant proteins are obtained from crude cell lysates.

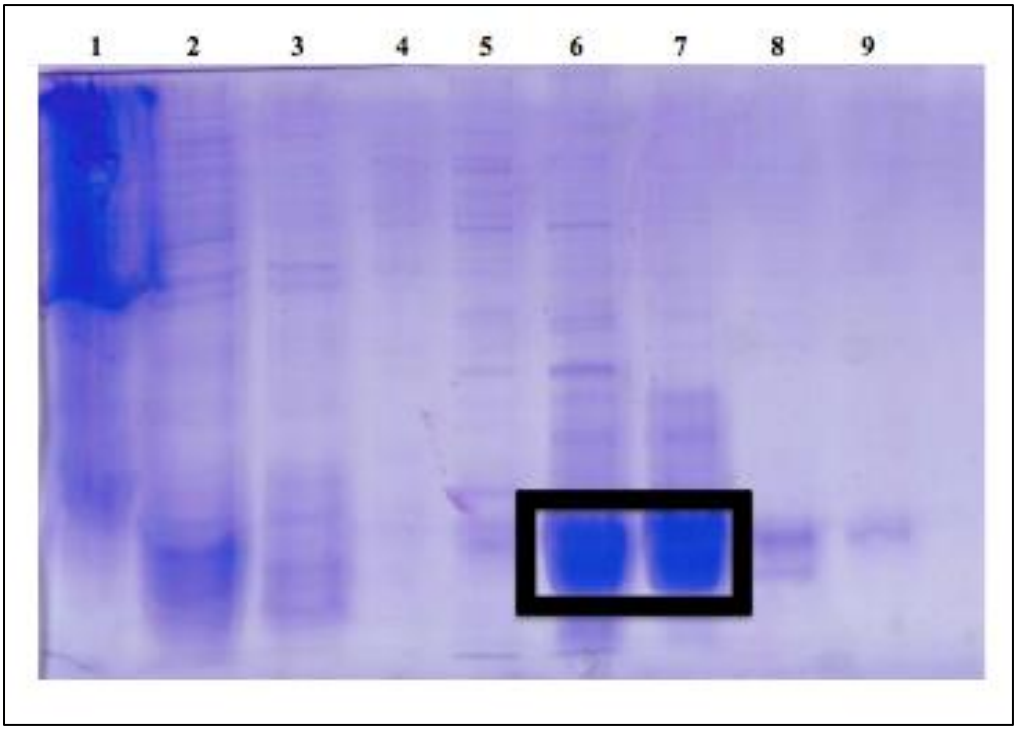

Figure C6. SDS-PAGE analysis of a purification of Rub-FGF1. The lanes correspond to Pellet (Lane-1), Supernatant (Lane-2), Flow-through (Lane-3), 20mM IMD (Lane-4), 50mM IMD (Lane-5), 100mM IMD (Lane-6), 250mM IMD (Lane-7), 500mM IMD (Lane-8) and Urea (Lane-9). The gel results show the successful expression and purification of Rub-FGF1 fusion protein corresponding to thick compact bands in lane-6 and 7 (boxed) at 100mM IMD and 250mM IMD, respectively.

The pure recombinant protein in this case Rub-FGF1 is eluted using different concentrations of imidazole (IMD). Imidazole competes with the his-tag for binding to the Ni^{+}-charged column. A range of low to high concentrations of imidazole is added. Proteins that bind weakly typically elute at lower concentrations of imidazole (20mM and 50mM IMD), where as His-tagged proteins are eluted at higher concentrations of imidazole (100mM and 250mM IMD).

If the his-tag is longer, a higher concentration of imidazole is required to elute bound proteins from the column. Using longer his-tags typically helps when there are more non-recombinant proteins present, especially if the recombinant protein is from a eukaryotic source.

The pH of the buffer used to prepare imidazole for elution was set at 7.2 (10X Phosphate Buffer Saline (PBS)), since it is consistent with the physiological pH. I used an established purification protocol in Kumar's lab and obtained pure compact protein at pH 7.2 and did not have to optimize my purification at different pHs.

Figure C7. Ni_+-NTA metal affinity purification setup. Rubredoxin provides a direct read-out for the expression and elution of the recombinant protein Rub-FGF1. The red color on the column is because of Rubredoxin.

Since my recombinant protein had a Rubredoxin upstream of the C-terminal heparin binding peptide of FGF1, purification was easy. Rubredoxin, a stable protein, provided a direct read-out of the expression and elution of the protein because of its red color. The recombinant protein could be seen eluting through the column. A lower flow-rate of 2ml/min was used to

achieve efficient elution of the recombinant protein. Figure C7 shows the purification setup and red color of the protein on the Ni+-NTA column.

4. <u>Concentration and Heat Treatment</u>

Figure C8 shows the results of protein concentration of the 250mM IMD fraction collected during purification. The fraction was concentrated to 5 ml with buffer exchange (1X PBS pH 7.2). Comparing lanes 2 and 3 in Figure C8 shows Rub-FGF1 concentration (boxed) pre- and post-concentration. A thicker, more compact Rub-FGF1 band is obtained as shown in Lane 3.

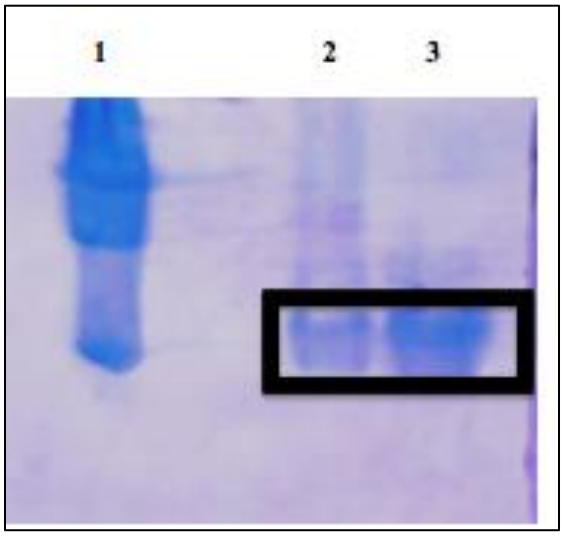

Figure C8. Concentration of purified Rub-FGF1. The lanes correspond to In-house Protein marker (Lane-1), Purified 250mM IMD fraction (Lane-2), Concentrated 250mM IMD purified sample (Lane-3).

Amicon Ultra Centrifugal filter was used to concentrate the recombinant protein. Through ultrafiltration, fast sample processing and efficient concentration of Rub-FGF1 was obtained for downstream experiments.

The SDS-PAGE for heat-treated concentrated sample is shown in Figure C9. The

objective of heat treatment was to obtain a pure compact band of Rub-FGF1 before using the sample for further experiments. As shown in the figure lane 3, post-heat treatment, most of the impurities in the 250mM IMD are left in the pellet. The pellet contains all the contaminants that are not resistant to heat. Rubredoxin-tagged recombinant protein however is thermostable and can be seen as a single pure band in the supernatant in lane 4.

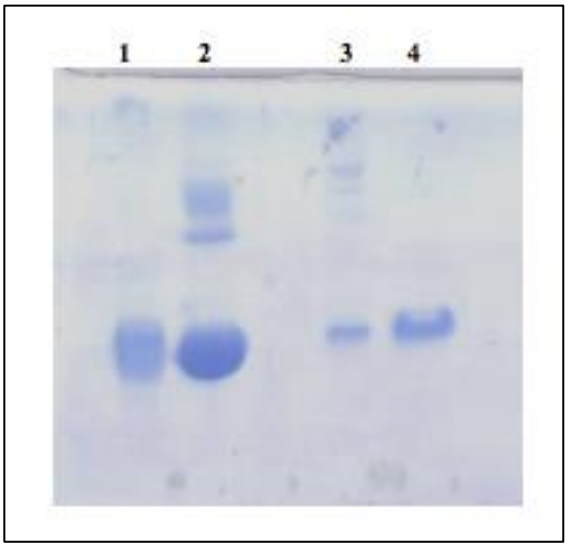

Figure C9. Heat Treatment of Purified, Concentrated 250mM IMD fraction. The lanes correspond to concentrated sample (Lane-1: same as Lane-3 in Figure C8.), Protein marker (Lane-2), Pellet (Lane-3) and Supernatant (Lane-4).

5, Thrombin Cleavage

The concentrated heat-treated pure 250mM IMD sample was cleaved by thrombin and processed. Thrombin cleaves at LVPR-GS at the junction of Rubredoxin and FGF1 C-terminal peptide. Lane 3 in Figure C10 represents the complete cleavage of Rub-FGF1 fused protein into Rub (7.15-kDa) and FGF1 peptide (2.75-kDa). After several optimizations for TCA preps, we were able to obtain pure FGF1 peptide with 7.5 % TCA prep as shown in Lane 6 in Figure C10.

TCA precipitation is a technique used for concentrating protein solutions and

simultaneously removes contaminating substances. 7.5% TCA precipitation was carried out on the thrombin cleaved Rub-FGF1 in order to get rid of Rubredoxin which stays in the pellet after TCA precipitation as shown in lane 5 of Figure C10.

The pure peptide was further characterized by mass spectrometry, analysis by circular dichroism (CD) and Fluorescence.

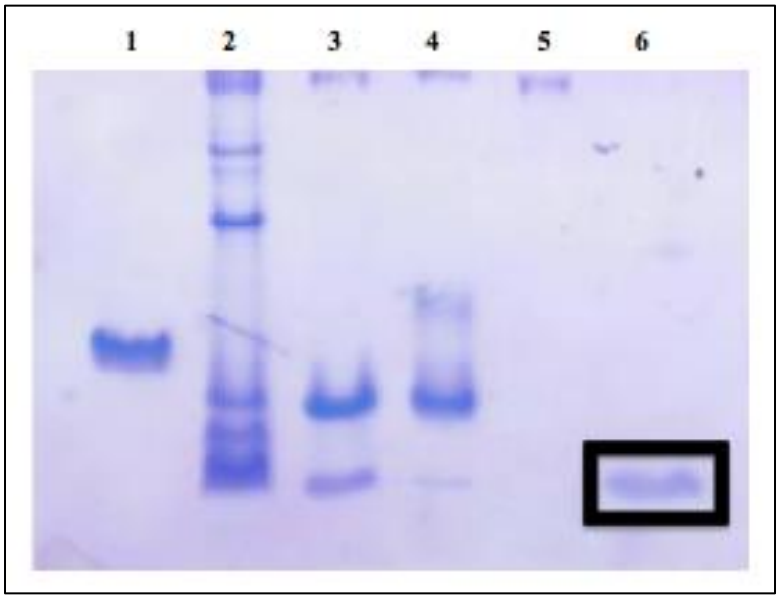

Figure C10. Thrombin Cleavage. The lanes correspond to Concentrated heat treated purified protein-2.69mg/ml (Lane-1), Direct thrombin cleavage pellet after heat treatment (Lane-2), Direct thrombin cleavage supernatant after heat treatment (Lane-3), 7.5% TCA prep-pellet dissolved in 1X PBS pH 7.2 (Lane-4), 7.5% TCA prep-supernatant 1ml heat treated-pellet (Lane-5), 7.5% TCA prep-supernatant 1ml heat treated-supernatant (Lane-6).

6. Circular Dichroism Spectroscopy

The CD spectrum in Figure C11 shows (based on comparison with standard curves) that FGF1 peptide is an α helix with positive peak at 190 nm and minima at 208 and 222 nm. According to literature, if the second minima (222nm) are shallower, the α helix has increasing amounts of random coil, which is shown in my data.

Circular Dichroism (CD) is a technique employed to determine the secondary structure of proteins. Different structural elements have characteristic CD spectra. It is due to the chromophores of the amides of the polypeptide backbones of proteins being aligned in arrays and shift in their optical transitions (Greenfield, 2006). α-helical proteins have minima at 222nm and 208nm and a positive maximum at 195nm (Greenfield, 2006). β-pleated sheets have a minimum at 218nm and a maximum at 195nm (Greenfield, 2006).

In order to determine the secondary structure of protein, the protein sample needs to at least 95% pure and the protein concentration may range from 0.005 to 5mg/ml (Greenfield, 2006). This can be obtained by HPLC or gel electrophoresis (Greenfield, 2006). Although CD doesn't provide secondary structure of specific residues as X-ray crystallography and NMR, it is advantageous because it allows data collection and analysis in less time with protein samples having concentrations as less as 20μg in aqueous buffers under physiological conditions (Greenfield, 2006).

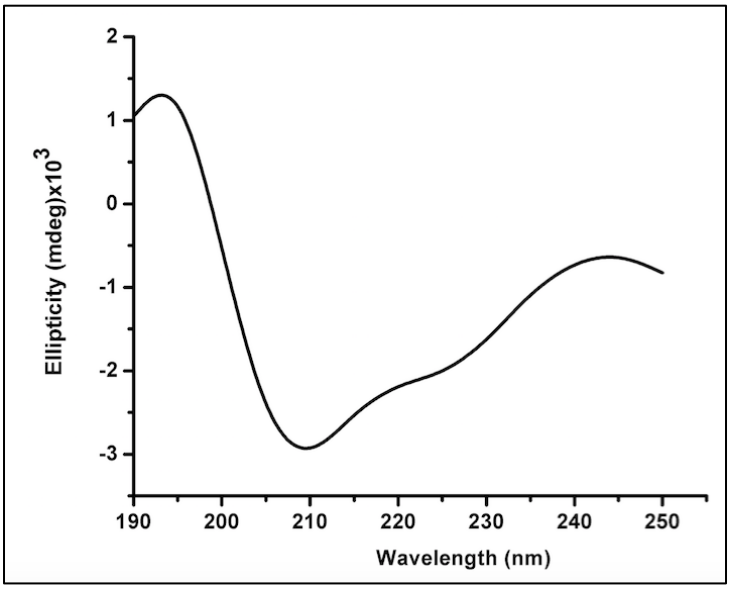

Figure C11. Circular Dichroism. CD spectrum of 0.87mg/ml FGF1 peptide reveals that it's a random coil.

7. **Fluorescence**

The fluorescence spectrum is in the range from 300-450 nm as shown in Figure C12. The excitation was set at 280nm. The emission wavelength as observed from the spectrum is at 350nm consistent with the presence of tryptophan in the heparin-binding pocket of FGF1.

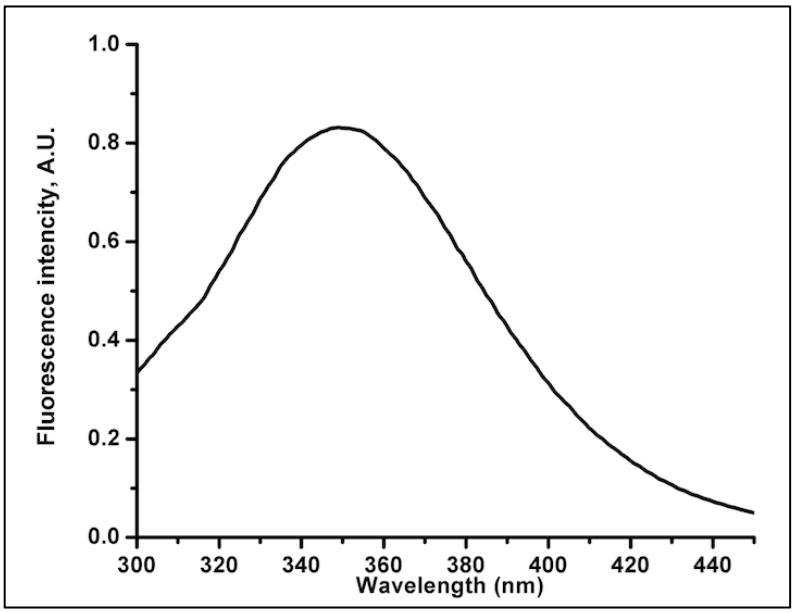

Figure C12. Fluorescence emission spectrum of heparin binding pocket of FGF1. Protein (0.87mg/ml) was in 1X PBS pH 7.2. The excitation wavelength was 280nm and the emission wavelength as observed is at 350nm.

8. **Mass spectrometry**

The mass spectrum shown in Figure C13 was obtained for the peptide shown in Lane 6 Figure C10. The black-circled part highlights the molecular weight of the heparin binding peptide of FGF1 consistent with the size of 2.75 kDa. There are a lot of other peaks observed in the spectrum and since we didn't analyze it so we cannot say for sure, but it might correspond to thrombin enzyme utilized to cleave Rub-FGF1.

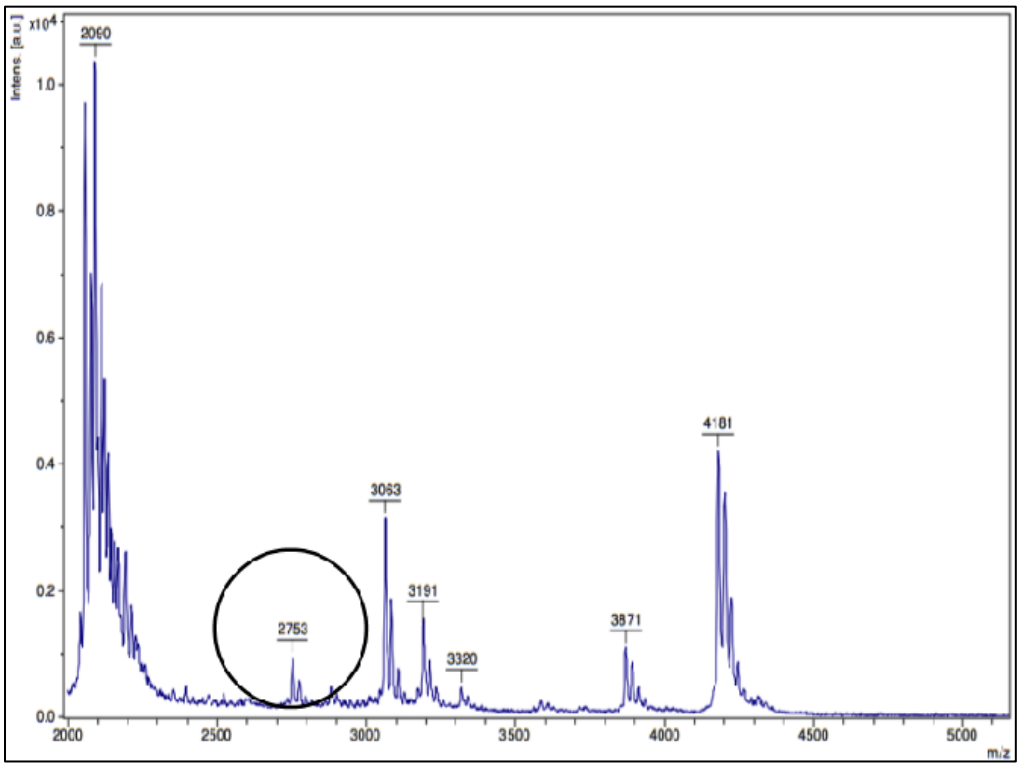

Figure C13. Mass Spectrometry Analysis of Heparin-Binding Peptide of FGF1. The circled part represents the molecular mass of heparin-binding peptide of FGF1 of 2.75-kDa.

9. Sequence Information

NNNNNGAGCCGGTACAATTCCCCTCTAGAAATAATTTTGTTTAACTTTAAGAAGGAG

ATATACATATGCACCACCACCACCACCACATGGCGAAATGGGTTTGCAAGATTTGCG

GCTATATTTACGACGAAGATGCTGGCGACCCGGACAACGGCATTAGTCCGGGCACC

AAATTTGAAGAACTGCCGGATGACTGGGTCTGCCCGATCTGTGGTGCGCCGAAAAG

CGAATTTGAAAAGCTGGAAGATCTGGTGCCGCGTGGATCCAACTGGTTCGTTGGTCT

GAAGAAAAACGGTTCGTGTAAACGCGGTCCGCGCACCCACTACGGTCAAAAATGAG

AATTCGAGCTCCGTCGACAAGCTTGCGGCCGCACTGGAGCACCACCACCACCACCA

CTGAGATCCGGCTGGTAACAAAGCCCGAAAGGAAGCTGGGTCGGCC

The sequence of Rub-FGF1 fusion protein is as follows:

Rub-FGF1

MHHHHHHMAKWVCKICGYIYDEDAGDPDNGISPGTKFEELPDDWVCPICGAPKSEFEK

LEDLVPRGSNWFVGLKKNGSCKRGPRTHYGQK

Rub protein

MHHHHHHMAKWVCKICGYIYDEDAGDPDNGISPGTKFEELPDDWVCPICGAPKSEFEK

LEDLVPR

FGF1 peptide

GSNWFVGLKKNGSCKRGPRTHYGQK

D. CONCLUSION

Several rounds of Ni^{+}-NTA purification of Rub-FGF1 resulted in stable Rub-FGF1 protein categorized by red color of Rubredoxin in solution. Heat-treatment to get rid of impurities showed that the fusion protein is stable to thermal degradation. Subjecting the fusion protein to cleavage by thrombin resulted in the separation of Rubredoxin and the heparin binding C-terminal pocket of FGF1. The important aspect of this project required obtaining pure heparin-binding C-terminal part of FGF1 and characterizing it. The heparin-binding part was successfully obtained by 7.5% TCA precipitation. HPLC was another technique to separate Rubredoxin and FGF1 post-thrombin cleavage (cleaves at LVPR-GS).

Circular Dichroism Spectroscopy of the heparin-binding peptide of FGF1 (25 amino acids long) showed increasing amount of random coil because of the shallow minima observed at 222 nm. Fluorescence spectroscopy data showed a maximum at 350nm consistent with the presence of tryptophan in the heparin-binding peptide of FGF1. A slight peak is observed at 308nm but it is not pronounced, however, its observation is consistent with the presence of tyrosine in the heparin-binding peptide of FGF1.

E. REFERENCES:

Bellosta, P., Iwahori, A., Plotnikov, A. N., Eliseenkova, A. V., Basilico, C., & Mohammadi, M. (2001). Identification of receptor and heparin binding sites in fibroblast growth factor 4 by structure-based mutagenesis. *Mol Cell Biol, 21*(17), 5946-5957.

Belov, A. A., & Mohammadi, M. (2013). Molecular mechanisms of fibroblast growth factor signaling in physiology and pathology. *Cold Spring Harb Perspect Biol, 5*(6). doi:10.1101/cshperspect.a015958

Bikfalvi, A., Klein, S., Pintucci, G., & Rifkin, D. B. (1997). Biological roles of fibroblast growth factor-2. *Endocr Rev, 18*(1), 26-45. doi:10.1210/edrv.18.1.0292

Blaber, M., DiSalvo, J., & Thomas, K. A. (1996). X-ray crystal structure of human acidic fibroblast growth factor. *Biochemistry, 35*(7), 2086-2094. doi:10.1021/bi9521755

DiGabriele, A. D., Lax, I., Chen, D. I., Svahn, C. M., Jaye, M., Schlessinger, J., & Hendrickson, W. A. (1998). Structure of a heparin-linked biologically active dimer of fibroblast growth factor. *Nature, 393*(6687), 812-817. doi:10.1038/31741

Esko, J. D., & Lindahl, U. (2001). Molecular diversity of heparan sulfate. *J Clin Invest, 108*(2), 169-173. doi:10.1172/JCI13530

Gallagher, J. T. (2001). Heparan sulfate: growth control with a restricted sequence menu. *J Clin Invest, 108*(3), 357-361. doi:10.1172/JCI13713

Greenfield, N. J. (2006). Using circular dichroism spectra to estimate protein secondary structure. *Nat Protoc, 1*(6), 2876-2890. doi:10.1038/nprot.2006.202

Itoh, N. (2007). The Fgf families in humans, mice, and zebrafish: their evolutional processes and roles in development, metabolism, and disease. *Biol Pharm Bull, 30*(10), 1819-1825.

Kan, M., Wang, F., To, B., Gabriel, J. L., & McKeehan, W. L. (1996). Divalent cations and heparin/heparan sulfate cooperate to control assembly and activity of the fibroblast growth factor receptor complex. *J Biol Chem, 271*(42), 26143-26148.

Kohli, B. M., & Ostermeier, C. (2003). A Rubredoxin based system for screening of protein expression conditions and on-line monitoring of the purification process. *Protein Expr Purif, 28*(2), 362-367.

Kreuger, J., Jemth, P., Sanders-Lindberg, E., Eliahu, L., Ron, D., Basilico, C., . . . Lindahl, U. (2005). Fibroblast growth factors share binding sites in heparan sulphate. *Biochem J, 389*(Pt 1), 145-150. doi:10.1042/BJ20042129

Mohammadi, M., Olsen, S. K., & Ibrahimi, O. A. (2005). Structural basis for fibroblast growth factor receptor activation. *Cytokine Growth Factor Rev, 16*(2), 107-137. doi:10.1016/j.cytogfr.2005.01.008

Muñoz, E. M., & Linhardt, R. J. (2004). Heparin-binding domains in vascular biology. *Arterioscler Thromb Vasc Biol, 24*(9), 1549-1557. doi:10.1161/01.ATV.0000137189.22999.3f

Ori, A., Free, P., Courty, J., Wilkinson, M. C., & Fernig, D. G. (2009). Identification of heparin-binding sites in proteins by selective labeling. *Mol Cell Proteomics, 8*(10), 2256-2265. doi:10.1074/mcp.M900031-MCP200

Ornitz, D. M., & Itoh, N. (2001). Fibroblast growth factors. *Genome Biol, 2*(3), REVIEWS3005.

Ornitz, D. M., & Itoh, N. (2015). The Fibroblast Growth Factor signaling pathway. *Wiley Interdiscip Rev Dev Biol, 4*(3), 215-266. doi:10.1002/wdev.176

Ostrovsky, O., Berman, B., Gallagher, J., Mulloy, B., Fernig, D. G., Delehedde, M., & Ron, D. (2002). Differential effects of heparin saccharides on the formation of specific fibroblast growth factor (FGF) and FGF receptor complexes. *J Biol Chem, 277*(4), 2444-2453. doi:10.1074/jbc.M108540200

Pellegrini, L., Burke, D. F., von Delft, F., Mulloy, B., & Blundell, T. L. (2000). Crystal structure of fibroblast growth factor receptor ectodomain bound to ligand and heparin. *Nature, 407*(6807), 1029-1034. doi:10.1038/35039551

Pineda-Lucena, A., Núñez De Castro, I., Lozano, R. M., Muñoz-Willery, I., Zazo, M., & Giménez-Gallego, G. (1994). Effect of low pH and heparin on the structure of acidic fibroblast growth factor. *Eur J Biochem, 222*(2), 425-431.

Plotnikov, A. N., Hubbard, S. R., Schlessinger, J., & Mohammadi, M. (2000). Crystal structures of two FGF-FGFR complexes reveal the determinants of ligand-receptor specificity. *Cell, 101*(4), 413-424.

Raman, R., Venkataraman, G., Ernst, S., Sasisekharan, V., & Sasisekharan, R. (2003). Structural specificity of heparin binding in the fibroblast growth factor family of proteins. *Proc Natl Acad Sci U S A, 100*(5), 2357-2362. doi:10.1073/pnas.0437842100

Stauber, D. J., DiGabriele, A. D., & Hendrickson, W. A. (2000). Structural interactions of fibroblast growth factor receptor with its ligands. *Proc Natl Acad Sci U S A, 97*(1), 49-54.

Steen, H., & Mann, M. (2004). The ABC's (and XYZ's) of peptide sequencing. *Nat Rev Mol Cell Biol, 5*(9), 699-711. doi:10.1038/nrm1468

Venkataraman, G., Shriver, Z., Davis, J. C., & Sasisekharan, R. (1999). Fibroblast growth factors 1 and 2 are distinct in oligomerization in the presence of heparin-like glycosaminoglycans. *Proc Natl Acad Sci U S A, 96*(5), 1892-1897.

Wong, P., Hampton, B., Szylobryt, E., Gallagher, A. M., Jaye, M., & Burgess, W. H. (1995). Analysis of putative heparin-binding domains of fibroblast growth factor-1. Using site-directed mutagenesis and peptide analogues. *J Biol Chem, 270*(43), 25805-25811.

Woodbury, M. E., & Ikezu, T. (2014). Fibroblast growth factor-2 signaling in neurogenesis and neurodegeneration. *J Neuroimmune Pharmacol, 9*(2), 92-101. doi:10.1007/s11481-013-9501-5

Yeh, B. K., Eliseenkova, A. V., Plotnikov, A. N., Green, D., Pinnell, J., Polat, T., . . . Mohammadi, M. (2002). Structural basis for activation of fibroblast growth factor signaling by sucrose octasulfate. *Mol Cell Biol, 22*(20), 7184-7192.